Understanding the nature of baryon resonances

Derek Leinweber

In collaboration with: Curtis Abell, Liam Hockley, Waseem Kamleh,
Yan Li, Zhan-Wei Liu, Finn Stokes, Tony Thomas, Jia-Jun Wu

The spectrum of a simple quark model: N and Λ baryons

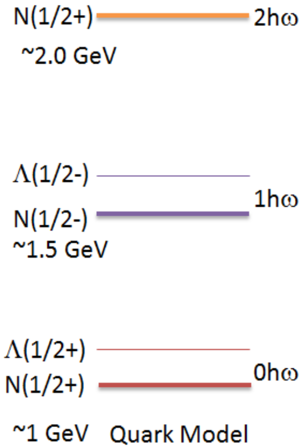

The challenge of experiment

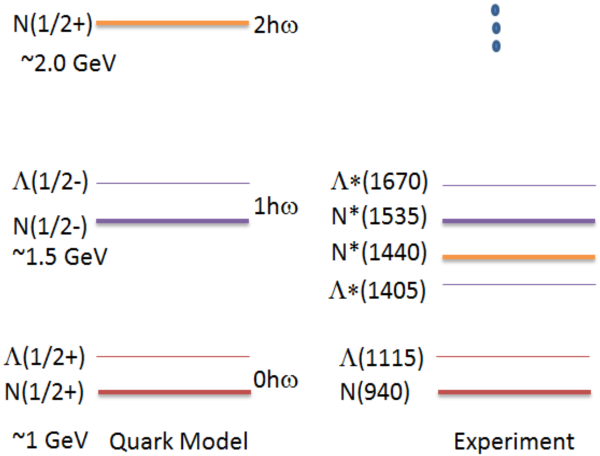

Prologue

- The idea of dressing quark-model states in a coupled-channel analysis to describe scattering data has been around for decades.

Prologue

- The idea of dressing quark-model states in a coupled-channel analysis to describe scattering data has been around for decades.
- What's new are formalisms able to bring these descriptions to the finite-volume of lattice QCD.

Prologue

- The idea of dressing quark-model states in a coupled-channel analysis to describe scattering data has been around for decades.
- What's new are formalisms able to bring these descriptions to the finite-volume of lattice QCD.
- Lattice QCD calculations of the excitation spectrum provide new constraints.

Prologue

- The idea of dressing quark-model states in a coupled-channel analysis to describe scattering data has been around for decades.
- What's new are formalisms able to bring these descriptions to the finite-volume of lattice QCD.
- Lattice QCD calculations of the excitation spectrum provide new constraints.
- It's time to reconsider our early notions about the quark-model and its excitation spectrum.

Outline

- Hamiltonian Effective Field Theory (HEFT)
  - Coupled-channel analysis technique aimed at resonance physics.
  - Incorporates the Lüscher formalism.
  - Connects scattering observables to the finite-volume spectrum of lattice QCD.

Outline

- Hamiltonian Effective Field Theory (HEFT)
  - Coupled-channel analysis technique aimed at resonance physics.
  - Incorporates the Lüscher formalism.
  - Connects scattering observables to the finite-volume spectrum of lattice QCD.
- Δ Resonance: introduce HEFT and illustrate the constraints provided by Lüscher.

Outline

- Hamiltonian Effective Field Theory (HEFT)
  - Coupled-channel analysis technique aimed at resonance physics.
  - Incorporates the Lüscher formalism.
  - Connects scattering observables to the finite-volume spectrum of lattice QCD.
- Δ Resonance: introduce HEFT and illustrate the constraints provided by Lüscher.
- $N^*(1535)$ and $N^*(1650)$ Resonances: novel two quark-model basis-state analysis.

Outline

- Hamiltonian Effective Field Theory (HEFT)
  - Coupled-channel analysis technique aimed at resonance physics.
  - Incorporates the Lüscher formalism.
  - Connects scattering observables to the finite-volume spectrum of lattice QCD.
- Δ Resonance: introduce HEFT and illustrate the constraints provided by Lüscher.
- $N^*(1535)$ and $N^*(1650)$ Resonances: novel two quark-model basis-state analysis.
- $\Lambda(1405)$ Resonance: evidence of a dominant $\overline{K}N$ component

Outline

- Hamiltonian Effective Field Theory (HEFT)
  - Coupled-channel analysis technique aimed at resonance physics.
  - Incorporates the Lüscher formalism.
  - Connects scattering observables to the finite-volume spectrum of lattice QCD.
- Δ Resonance: introduce HEFT and illustrate the constraints provided by Lüscher.
- $N^*(1535)$ and $N^*(1650)$ Resonances: novel two quark-model basis-state analysis.
- $\Lambda(1405)$ Resonance: evidence of a dominant $\overline{K}N$ component
- Roper $N(1440)$ Resonance:
  - Lattice QCD results constrain the HEFT description of experimental data.
  - Poses a new resolution of the missing baryon resonances problem.

Hamiltonian Effective Field Theory (HEFT)

J. M. M. Hall, *et al.* [CSSM], Phys. Rev. D **87** (2013) 094510 [arXiv:1303.4157 [hep-lat]]

C. D. Abell, DBL, A. W. Thomas, J. J. Wu, Phys. Rev. D **106** (2022) 034506 [arXiv:2110.14113 [hep-lat]]

- An extension of chiral effective field theory incorporating the Lüscher formalism
  - Linking the energy levels observed in finite volume to scattering observables.

Hamiltonian Effective Field Theory (HEFT)

J. M. M. Hall, *et al.* [CSSM], Phys. Rev. D **87** (2013) 094510 [arXiv:1303.4157 [hep-lat]]

C. D. Abell, DBL, A. W. Thomas, J. J. Wu, Phys. Rev. D **106** (2022) 034506 [arXiv:2110.14113 [hep-lat]]

- An extension of chiral effective field theory incorporating the Lüscher formalism
  - Linking the energy levels observed in finite volume to scattering observables.
- In the light quark-mass regime, in the perturbative limit,
  - HEFT reproduces the finite-volume expansion of chiral perturbation theory.

Hamiltonian Effective Field Theory (HEFT)

J. M. M. Hall, *et al.* [CSSM], Phys. Rev. D **87** (2013) 094510 [arXiv:1303.4157 [hep-lat]]

C. D. Abell, DBL, A. W. Thomas, J. J. Wu, Phys. Rev. D **106** (2022) 034506 [arXiv:2110.14113 [hep-lat]]

- An extension of chiral effective field theory incorporating the Lüscher formalism
  - Linking the energy levels observed in finite volume to scattering observables.
- In the light quark-mass regime, in the perturbative limit,
  - HEFT reproduces the finite-volume expansion of chiral perturbation theory.
- Fitting resonance phase-shift data and inelasticities,
  - Predictions of the finite-volume spectrum are made.

Hamiltonian Effective Field Theory (HEFT)

J. M. M. Hall, *et al.* [CSSM], Phys. Rev. D **87** (2013) 094510 [arXiv:1303.4157 [hep-lat]]

C. D. Abell, DBL, A. W. Thomas, J. J. Wu, Phys. Rev. D **106** (2022) 034506 [arXiv:2110.14113 [hep-lat]]

- An extension of chiral effective field theory incorporating the Lüscher formalism
  - Linking the energy levels observed in finite volume to scattering observables.
- In the light quark-mass regime, in the perturbative limit,
  - HEFT reproduces the finite-volume expansion of chiral perturbation theory.
- Fitting resonance phase-shift data and inelasticities,
  - Predictions of the finite-volume spectrum are made.
- The eigenvectors of the Hamiltonian provide insight into the composition of the energy eigenstates.
  - Insight is similar to that provided by correlation-matrix eigenvectors in Lattice QCD.

Infinite Volume Model

- The rest-frame Hamiltonian has the form $H = H_0 + H_I$, with

$$H_0 = \sum_{B_0} |B_0\rangle\, m_{B_0}\, \langle B_0| + \sum_{\alpha} \int d^3k\, |\alpha(\boldsymbol{k})\rangle\, \omega_\alpha(\boldsymbol{k})\, \langle \alpha(\boldsymbol{k})| \,,$$

Infinite Volume Model

- The rest-frame Hamiltonian has the form $H = H_0 + H_I$, with

$$H_0 = \sum_{B_0} |B_0\rangle\, m_{B_0}\, \langle B_0| + \sum_{\alpha} \int d^3k\, |\alpha(\boldsymbol{k})\rangle\, \omega_\alpha(\boldsymbol{k})\, \langle \alpha(\boldsymbol{k})| \,,$$

- $|B_0\rangle$ denotes a quark-model-like basis state with bare mass m_{B_0}.

Infinite Volume Model

- The rest-frame Hamiltonian has the form $H = H_0 + H_I$, with

$$H_0 = \sum_{B_0} |B_0\rangle\, m_{B_0}\, \langle B_0| + \sum_{\alpha} \int d^3k\, |\alpha(\boldsymbol{k})\rangle\, \omega_\alpha(\boldsymbol{k})\, \langle \alpha(\boldsymbol{k})| \,,$$

- $|B_0\rangle$ denotes a quark-model-like basis state with bare mass m_{B_0}.
- $|\alpha(\boldsymbol{k})\rangle$ designates a two-particle non-interacting basis-state channel with energy

$$\omega_\alpha(\boldsymbol{k}) = \omega_{\alpha_M}(\boldsymbol{k}) + \omega_{\alpha_B}(\boldsymbol{k}) = \sqrt{\boldsymbol{k}^2 + m_{\alpha_M}^2} + \sqrt{\boldsymbol{k}^2 + m_{\alpha_B}^2} \,,$$

for $M =$ Meson, $B =$ Baryon.

Infinite Volume Model

- The interaction Hamiltonian includes two parts, $H_I = g + v$.
- $1 \to 2$ particle vertex

$$g = \sum_{\alpha,\, B_0} \int d^3k \, \left\{ \, |\alpha(\boldsymbol{k})\rangle \, G^{\dagger}_{\alpha,B_0}(k) \, \langle B_0| + h.c. \right\} \, ,$$

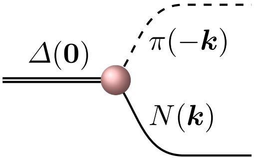

Infinite Volume Model

- The interaction Hamiltonian includes two parts, $H_I = g + v$.
- $1 \to 2$ particle vertex

$$g = \sum_{\alpha,\, B_0} \int d^3k \, \left\{ |\alpha(\boldsymbol{k})\rangle \, G^{\dagger}_{\alpha,B_0}(k) \, \langle B_0| + h.c. \right\} \, ,$$

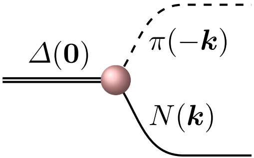

- $2 \to 2$ particle vertex

$$v = \sum_{\alpha,\beta} \int d^3k \; d^3k' \, |\alpha(\boldsymbol{k})\rangle \, V^S_{\alpha,\beta}(k,k') \, \langle \beta(\boldsymbol{k}')| \, .$$

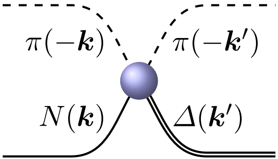

S-wave vertex interactions

- S-wave vertex interactions between the one baryon and two-particle meson-baryon channels for e.g. $N^*(1535)$ or $\Lambda^*(1405)$ cases take the form

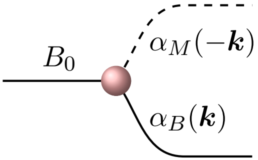

$$G_{\alpha,B_0}(k) = g_{B_0\alpha}\, \frac{\sqrt{3}}{2\,\pi\, f_\pi}\, \sqrt{\omega_{\alpha_M}(k)}\, u(k,\Lambda)\,,$$

with regulator

$$u(k,\Lambda) = \left(1 + \frac{k^2}{\Lambda^2}\right)^{-2}\,.$$

P-wave and higher vertex interactions

- P-wave and higher vertex interactions for the $\Delta(1232)$ or $N^*(1440)$ take the form

$$G_{\alpha,B_0}(k) = g_{B_0\alpha}\,\frac{1}{4\pi^2}\left(\frac{k}{f_\pi}\right)^{l_\alpha}\frac{u(k,\Lambda)}{\sqrt{\omega_{\alpha_M}(k)}}\,,$$

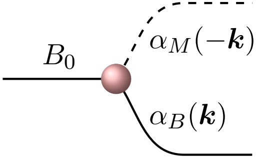

where l_α is the orbital angular momentum in channel α.

Two-to-two particle interactions

- For the direct two-to-two particle interaction, we introduce separable potentials.

Two-to-two particle interactions

- For the direct two-to-two particle interaction, we introduce separable potentials.
- For the S_{11} πN channel

$$V^{S}_{\pi N,\pi N}\,(\,k,\;k'\,) = v_{\pi N,\pi N}\,\frac{3}{4\pi^2\,f_\pi^2}\,\tilde{u}_{\pi N}(k,\Lambda)\,\tilde{u}_{\pi N}(k',\Lambda)$$

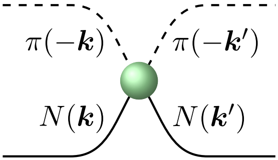

where the scattering potential gains a low energy enhancement via

$$\tilde{u}_{\pi N}(k,\Lambda) = u(k,\Lambda)\,\frac{m_\pi^{\text{phys}} + \omega_\pi(k)}{\omega_\pi(k)}$$

and $u(k,\Lambda)$ takes the dipole form.

Two-to-two particle interactions

- For P-wave scattering in the $\Delta(1232)$ or $N^*(1440)$ channels

$$V^S_{\alpha,\beta}\,(\,k,\,k'\,) = v_{\alpha,\beta}\,\frac{1}{4\pi^2\,f_\pi^2}\,\frac{k}{\omega_{\alpha_M}(k)}\,\frac{k'}{\omega_{\beta_M}(k')}\,u(k,\Lambda)\,u(k',\Lambda)\,.$$

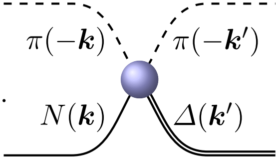

Two-to-two particle interactions

- For P-wave scattering in the $\Delta(1232)$ or $N^*(1440)$ channels

$$V^S_{\alpha,\beta}(k,\,k') = v_{\alpha,\beta}\,\frac{1}{4\pi^2 f_\pi^2}\,\frac{k}{\omega_{\alpha_M}(k)}\,\frac{k'}{\omega_{\beta_M}(k')}\,u(k,\Lambda)\,u(k',\Lambda)\,.$$

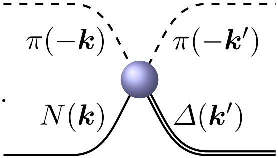

- For the $\Lambda^*(1405)$, the Weinberg-Tomozawa term is considered

$$V^S_{\alpha,\beta}(k,\,k') = g^{\Lambda^*}_{\alpha,\beta}\,\frac{[\,\omega_{\alpha_M}(k)+\omega_{\beta_M}(k')\,]\,u(k,\Lambda)\,u(k',\Lambda)}{16\,\pi^2 f_\pi^2\sqrt{\omega_{\alpha_M}(k)\,\omega_{\beta_M}(k')}}\,,$$

Infinite-Volume scattering amplitude

- The T-matrices for two particle scattering are obtained by solving the coupled-channel integral equations

$$T_{\alpha,\beta}(k,k';E) = \tilde{V}_{\alpha,\beta}(k,k';E) + \sum_{\gamma} \int q^2 dq \, \frac{\tilde{V}_{\alpha,\gamma}(k,q;E)\, T_{\gamma,\beta}(q,k';E)}{E - \omega_\gamma(q) + i\epsilon} \,.$$

Infinite-Volume scattering amplitude

- The T-matrices for two particle scattering are obtained by solving the coupled-channel integral equations

$$T_{\alpha,\beta}(k,k';E) = \tilde{V}_{\alpha,\beta}(k,k';E) + \sum_{\gamma} \int q^2 dq \, \frac{\tilde{V}_{\alpha,\gamma}(k,q;E)\, T_{\gamma,\beta}(q,k';E)}{E - \omega_\gamma(q) + i\epsilon} \, .$$

- The coupled-channel potential is readily calculated from the interaction Hamiltonian

$$\tilde{V}_{\alpha,\beta}(k,k') = \sum_{B_0} \frac{G^{\dagger}_{\alpha,B_0}(k)\, G_{\beta,B_0}(k')}{E - m_{B_0}} + V^{S}_{\alpha,\beta}(k,k') \, ,$$

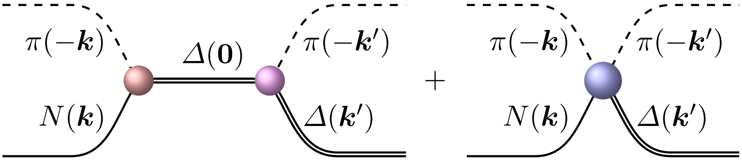

Infinite-Volume scattering matrix

- The S-matrix is related to the T-matrix by

$$S_{\alpha,\beta}(E) = 1 - 2i\sqrt{\rho_\alpha(E)\,\rho_\beta(E)}\;T_{\alpha,\beta}(k_{\alpha\,\mathrm{cm}}, k_{\beta\,\mathrm{cm}}; E)\,,$$

with

$$\rho_\alpha(E) = \pi\frac{\omega_{\alpha_M}(k_{\alpha\,\mathrm{cm}})\,\omega_{\alpha_B}(k_{\alpha\,\mathrm{cm}})}{E}\,k_{\alpha\,\mathrm{cm}}\,,$$

and $k_{\alpha\,\mathrm{cm}}$ satisfies the on-shell condition

$$\omega_{\alpha_M}(k_{\alpha\,\mathrm{cm}}) + \omega_{\alpha_B}(k_{\alpha\,\mathrm{cm}}) = E\,.$$

Infinite-Volume scattering matrix

- The S-matrix is related to the T-matrix by

$$S_{\alpha,\beta}(E) = 1 - 2i\,\sqrt{\rho_\alpha(E)\,\rho_\beta(E)}\;T_{\alpha,\beta}(k_{\alpha\,\mathrm{cm}}, k_{\beta\,\mathrm{cm}}; E)\,,$$

  with

$$\rho_\alpha(E) = \pi\frac{\omega_{\alpha_M}(k_{\alpha\,\mathrm{cm}})\,\omega_{\alpha_B}(k_{\alpha\,\mathrm{cm}})}{E}\;k_{\alpha\,\mathrm{cm}}\,,$$

  and $k_{\alpha\,\mathrm{cm}}$ satisfies the on-shell condition

$$\omega_{\alpha_M}(k_{\alpha\,\mathrm{cm}}) + \omega_{\alpha_B}(k_{\alpha\,\mathrm{cm}}) = E\,.$$

- The cross section $\sigma_{\alpha\,,\beta}$ for the process $\alpha \to \beta$ is

$$\sigma_{\alpha\,,\beta} = \frac{4\pi^3\,k_{\alpha\,\mathrm{cm}}\,\omega_{\alpha_M}(k_{\alpha\,\mathrm{cm}})\,\omega_{\alpha_B}(k_{\alpha\,\mathrm{cm}})\,\omega_{\beta_M}(k_{\alpha\,\mathrm{cm}})\,\omega_{\beta_B}(k_{\alpha\,\mathrm{cm}})}{E^2\,k_{\beta\,\mathrm{cm}}}\;\left|T_{\alpha,\beta}(k_{\alpha\,\mathrm{cm}}, k_{\beta\,\mathrm{cm}}; E)\right|^2\,.$$

πN phase shift and inelasticity

- The S-matrix is related to the T-matrix by

$$
\begin{aligned}
S_{\pi N,\pi N}(E) &= 1 - 2i\pi \frac{\omega_\pi(k_{\rm cm})\,\omega_N(k_{\rm cm})}{E}\, k_{\rm cm}\; T_{\pi N,\pi N}(k_{\rm cm}, k_{\rm cm}; E)\,, \\
&= \eta(E)\, e^{2i\,\delta(E)}\,.
\end{aligned}
$$

- In solving for the energy eigenstates. . .

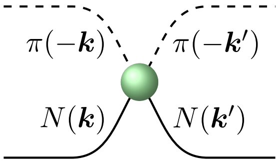

πN phase shift and inelasticity

- The S-matrix is related to the T-matrix by

$$\begin{aligned} S_{\pi N,\pi N}(E) &= 1 - 2i\pi \frac{\omega_\pi(k_{\rm cm})\,\omega_N(k_{\rm cm})}{E}\, k_{\rm cm}\; T_{\pi N,\pi N}(k_{\rm cm}, k_{\rm cm}; E)\,, \\ &= \eta(E)\, e^{2i\,\delta(E)}\,. \end{aligned}$$

- In solving for the energy eigenstates. . .

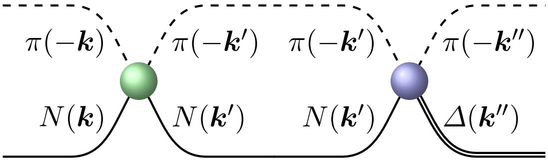

πN phase shift and inelasticity

- The S-matrix is related to the T-matrix by

$$\begin{aligned} S_{\pi N,\pi N}(E) &= 1 - 2i\pi \frac{\omega_\pi(k_{\rm cm})\,\omega_N(k_{\rm cm})}{E}\, k_{\rm cm}\; T_{\pi N,\pi N}(k_{\rm cm}, k_{\rm cm}; E)\,, \\ &= \eta(E)\, e^{2i\,\delta(E)}\,. \end{aligned}$$

- In solving for the energy eigenstates. . .

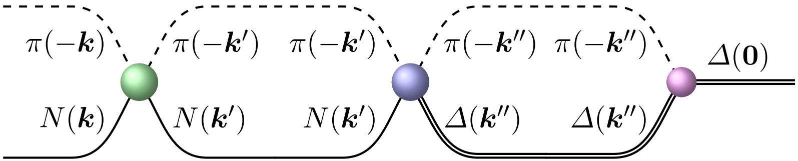

πN phase shift and inelasticity

- The S-matrix is related to the T-matrix by

$$
\begin{aligned}
S_{\pi N,\pi N}(E) &= 1 - 2i\pi \frac{\omega_\pi(k_{\rm cm})\,\omega_N(k_{\rm cm})}{E}\, k_{\rm cm}\; T_{\pi N,\pi N}(k_{\rm cm}, k_{\rm cm}; E)\,, \\
&= \eta(E)\, e^{2i\,\delta(E)}\,.
\end{aligned}
$$

- In solving for the energy eigenstates. . .

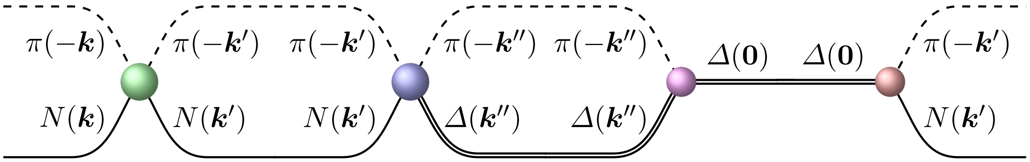

P-wave πN scattering in the Δ channel - 2 channel πN and $\pi\Delta$

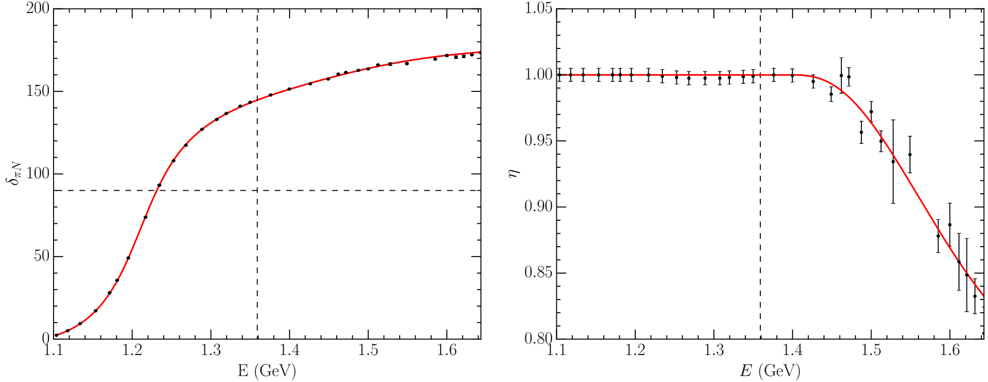

P-wave πN scattering in the Δ channel - 2 channel πN and $\pi\Delta$

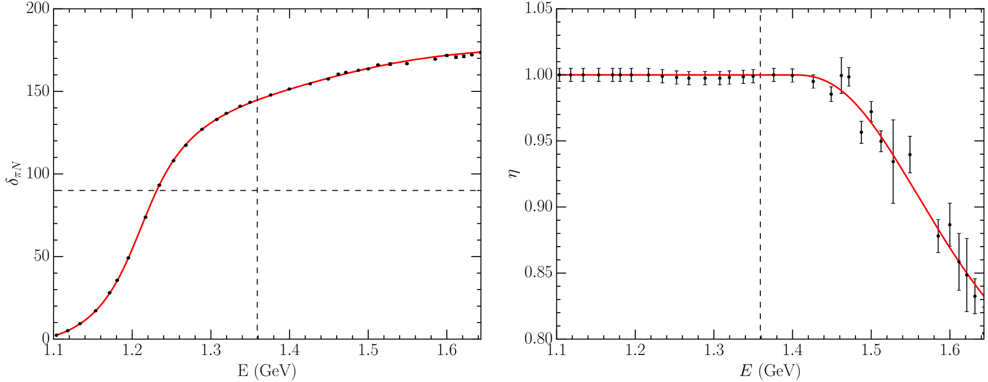

- Here $\Lambda = 0.8$ GeV, but $0.6 \leq \Lambda \leq 1.2$ GeV is acceptable.

Finite Volume Analysis - Hamiltonian Matrix

- In a finite periodic volume, momentum is quantised to $n\,(2\pi/L)$.

Finite Volume Analysis - Hamiltonian Matrix

- In a finite periodic volume, momentum is quantised to $n\,(2\pi/L)$.
- In a cubic volume of extent L on each side, define the momentum magnitudes

$$k_n = \sqrt{n_x^2 + n_y^2 + n_z^2}\,\frac{2\pi}{L}\,,$$

with $n_i = 0, 1, 2, \ldots$ and integer $n = n_x^2 + n_y^2 + n_z^2$.

Finite Volume Analysis - Hamiltonian Matrix

- In a finite periodic volume, momentum is quantised to $n\,(2\pi/L)$.
- In a cubic volume of extent L on each side, define the momentum magnitudes

$$k_n = \sqrt{n_x^2 + n_y^2 + n_z^2}\,\frac{2\pi}{L}\,,$$

  with $n_i = 0, 1, 2, \ldots$ and integer $n = n_x^2 + n_y^2 + n_z^2$.
- The degeneracy of each k_n is described by $C_3(n)$, which counts the number of ways the integers n_x, n_y, and n_z, can be squared and summed to n.

Finite Volume Analysis - Hamiltonian Matrix

- In a finite periodic volume, momentum is quantised to $n\,(2\pi/L)$.
- In a cubic volume of extent L on each side, define the momentum magnitudes

$$k_n = \sqrt{n_x^2 + n_y^2 + n_z^2}\,\frac{2\pi}{L}\,,$$

with $n_i = 0, 1, 2, \ldots$ and integer $n = n_x^2 + n_y^2 + n_z^2$.

- The degeneracy of each k_n is described by $C_3(n)$, which counts the number of ways the integers n_x, n_y, and n_z, can be squared and summed to n.
- The non-interacting Hamiltonian takes the form

$$H_0 = \mathrm{diag}(m_{B_0},\ \omega_{\pi N}(k_0),\ \omega_{\pi\Delta}(k_0),\ \omega_{\pi N}(k_1),\ \omega_{\pi\Delta}(k_1),\ \ldots)$$

Interaction Hamiltonian Terms

- $1 \to 2$ particle interaction terms sit in the first row and column.

$$H_I = \begin{pmatrix} 0 & \overline{G}_{\pi N, B_0}(k_0) & \cdots & \overline{G}_{\pi\Delta, B_0}(k_0) & \overline{G}_{\pi N, B_0}(k_1) & \cdots & \overline{G}_{\pi\Delta, B_0}(k_1) \cdots \\ \overline{G}^{\dagger}_{\pi N, B_0}(k_0) & 0 & & & & & \\ \vdots & & 0 & & & & \\ \overline{G}^{\dagger}_{\pi\Delta, B_0}(k_0) & & & \ddots & & & \\ \overline{G}^{\dagger}_{\pi N, B_0}(k_1) & & & & & & \\ \vdots & & & & & & \\ \overline{G}^{\dagger}_{\pi\Delta, B_0}(k_1) & & & & & & \\ \vdots & & & & & & \end{pmatrix} .$$

- $\cdots$ allow for additional channels.

Interaction Hamiltonian Terms

- $1 \to 2$ particle interaction terms sit in the first row and column.

$$H_I = \begin{pmatrix} 0 & \overline{G}_{\pi N, B_0}(k_0) & \cdots & \overline{G}_{\pi \Delta, B_0}(k_0) & \overline{G}_{\pi N, B_0}(k_1) & \cdots & \overline{G}_{\pi \Delta, B_0}(k_1) \cdots \\ \overline{G}^{\dagger}_{\pi N, B_0}(k_0) & 0 & & & & & \\ \vdots & & 0 & & & & \\ \overline{G}^{\dagger}_{\pi \Delta, B_0}(k_0) & & & \ddots & & & \\ \overline{G}^{\dagger}_{\pi N, B_0}(k_1) & & & & & & \\ \vdots & & & & & & \\ \overline{G}^{\dagger}_{\pi \Delta, B_0}(k_1) & & & & & & \\ \vdots & & & & & & \end{pmatrix} .$$

- $\cdots$ allow for additional channels.
- $2 \to 2$ particle interaction terms, $\overline{V}^{S}_{\alpha,\beta}(k_n, k_{n'})$, fill out the rest of the matrix.

Relation to infinite-volume contributions

- The finite volume Hamiltonian interaction terms are related to the infinite-volume contributions via

$$\int k^2 dk = \frac{1}{4\pi}\int d^3k \to \frac{1}{4\pi}\sum_{\boldsymbol{n}\in\mathbb{Z}^3}\left(\frac{2\pi}{L}\right)^3 = \frac{1}{4\pi}\sum_{n\in\mathbb{Z}} C_3(n)\left(\frac{2\pi}{L}\right)^3 .$$

such that

$$\bar{G}_{\alpha,B_0}(k_n) = \sqrt{\frac{C_3(n)}{4\pi}}\left(\frac{2\pi}{L}\right)^{\frac{3}{2}} G_{\alpha,B_0}(k_n)\,,$$

$$\bar{V}^S_{\alpha\beta}(k_n,k_m) = \sqrt{\frac{C_3(n)}{4\pi}}\sqrt{\frac{C_3(m)}{4\pi}}\left(\frac{2\pi}{L}\right)^3 V^S_{\alpha\beta}(k_n,k_m)\,.$$

Finite Volume Eigenmode Solution

- Standard Lapack routines provide eigenmode solutions of

$$\langle\, i \,|\, H \,|\, j \,\rangle\, \langle\, j \,|\, E_\alpha \,\rangle = E_\alpha \,\langle\, i \,|\, E_\alpha \,\rangle \,,$$

  - where $|\, i \,\rangle$ and $|\, j \,\rangle$ are the non-interacting basis states,
  - E_α is the energy eigenvalue, and
  - $\langle\, i \,|\, E_\alpha \,\rangle$ is the eigenvector of the
  - Hamiltonian matrix $\langle\, i \,|\, H \,|\, j \,\rangle$.

Mass dependence of energy eigenstates - Fit to PACS-CS Δ masses

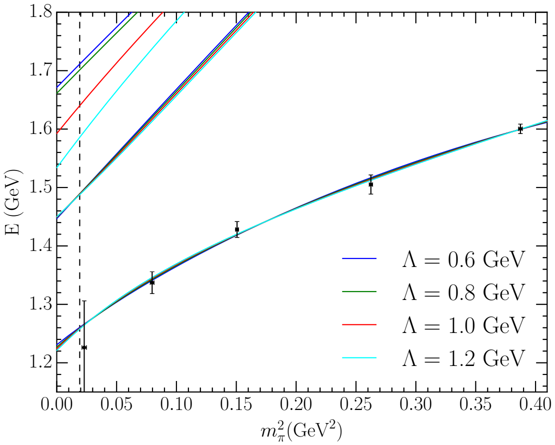

- Physical results extended via $m_0 \to m_0(m_\pi^2)$.

Mass dependence of energy eigenstates - Fit to PACS-CS Δ masses

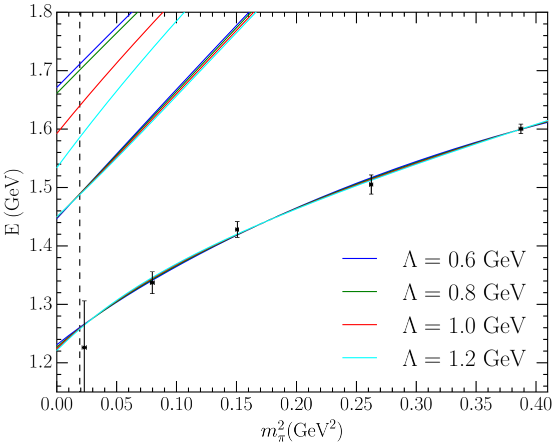

- Physical results extended via $m_0 \to m_0(m_\pi^2)$.
- Lattice QCD results can constrain the Hamiltonian description of experimental data.

New examination of low-lying odd-parity nucleon resonances

- Motivated by lattice QCD calculations of the electromagnetic form factors of the two low-lying odd-parity states.

  F. M. Stokes, W. Kamleh, DBL, Phys. Rev. D **102** (2020) 014507 [arXiv:1907.00177 [hep-lat]].

- Confirms quark model predictions for N^* magnetic moments.

N^* Magnetic Moments and the constituent quark model $m_\pi = 702$ MeV

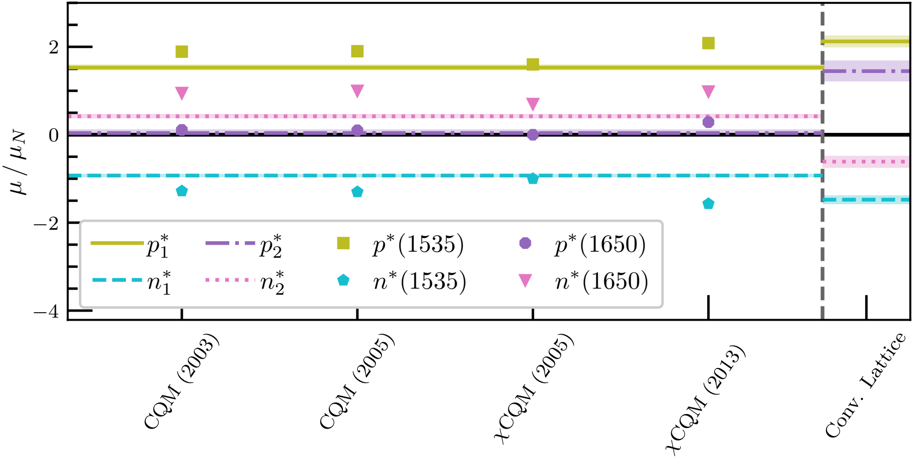

F. M. Stokes, W. Kamleh, DBL, Phys. Rev. D **102** (2020) 014507 [arXiv:1907.00177 [hep-lat]].

Model Calculation References

- CQM (2003)

  W.-T. Chiang, S. N. Yang, M. Vanderhaeghen, and D. Drechsel, Magnetic dipole moment of the S 11 (1535) from the $\gamma p \to \gamma \eta p$ reaction, Nucl. Phys. **A723**, 205 (2003), nucl-th/0211061

- χCQM (2005)

  J. Liu, J. He, and Y. Dong, Magnetic moments of negative-parity low-lying nucleon resonances in quark models, Phys. Rev. **D71**, 094004 (2005).

- χCQM (2013)

  N. Sharma, A. Martinez Torres, K. Khemchandani, and H. Dahiya, Magnetic moments of the low-lying $1/2^-$ octet baryon resonances, Eur. Phys. J. **A49**, 11 (2013), arXiv:1207.3311

New examination of low-lying odd-parity nucleon resonances

- Both the $N^*(1535)$ and $N^*(1650)$ are quark-model like at larger quark masses.

New examination of low-lying odd-parity nucleon resonances

- Both the $N^*(1535)$ and $N^*(1650)$ are quark-model like at larger quark masses.
- Introduce two bare basis states which mix to form the $N^*(1535)$ and $N^*(1650)$.

New examination of low-lying odd-parity nucleon resonances

- Both the $N^*(1535)$ and $N^*(1650)$ are quark-model like at larger quark masses.
- Introduce two bare basis states which mix to form the $N^*(1535)$ and $N^*(1650)$.
- Resonance decay properties demand πN, ηN, and $K\Lambda$ scattering channels.

New examination of low-lying odd-parity nucleon resonances

- Both the $N^*(1535)$ and $N^*(1650)$ are quark-model like at larger quark masses.
- Introduce two bare basis states which mix to form the $N^*(1535)$ and $N^*(1650)$.
- Resonance decay properties demand πN, ηN, and $K\Lambda$ scattering channels.
- 21 parameter fit provides an excellent characterisation of the data.
  - Pole positions agree with PDG.

Phase shift and inelasticity for the low-lying odd-parity spin-1/2 nucleon resonances

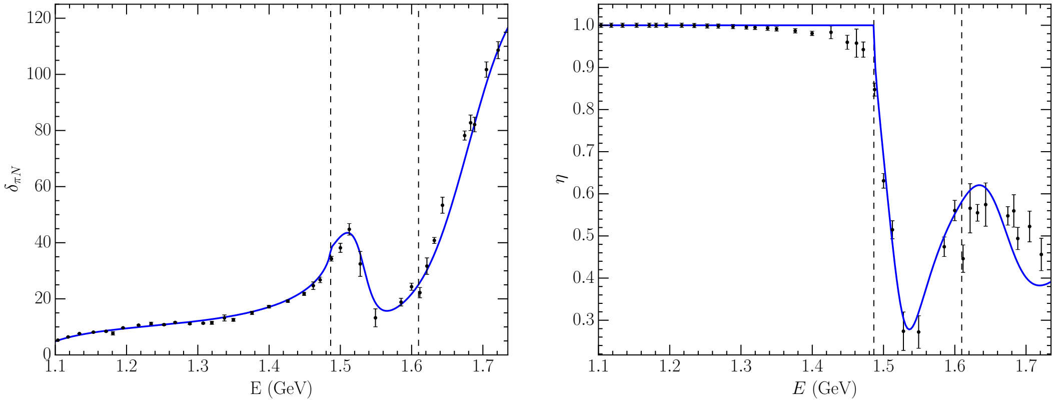

- WI08 single-energy data from SAID.
- Vertical lines indicate the opening of the ηN and $K\Lambda$ thresholds.

Phase shift and inelasticity for the low-lying odd-parity spin-1/2 nucleon resonances

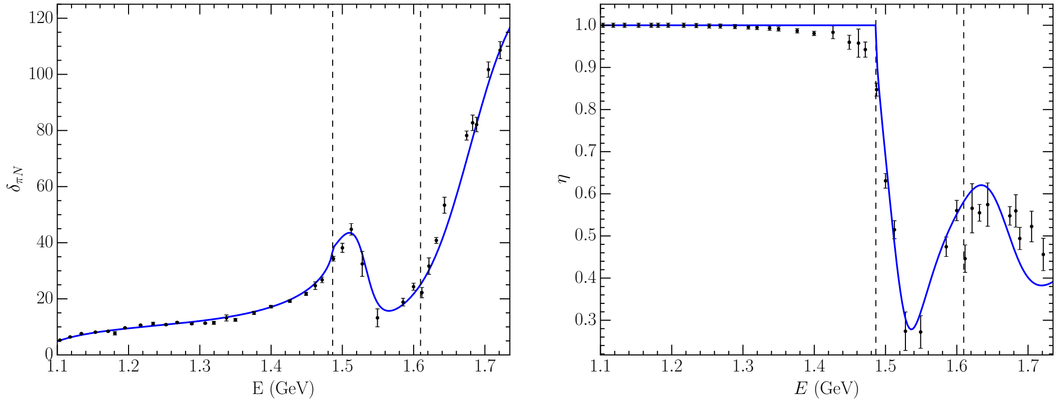

- WI08 single-energy data from SAID.
- Note the three-body $\pi\pi N$ threshold at 1.22 GeV.

Finite-volume $L = 3$ fm energy levels for low-lying odd-parity spin-1/2 nucleons

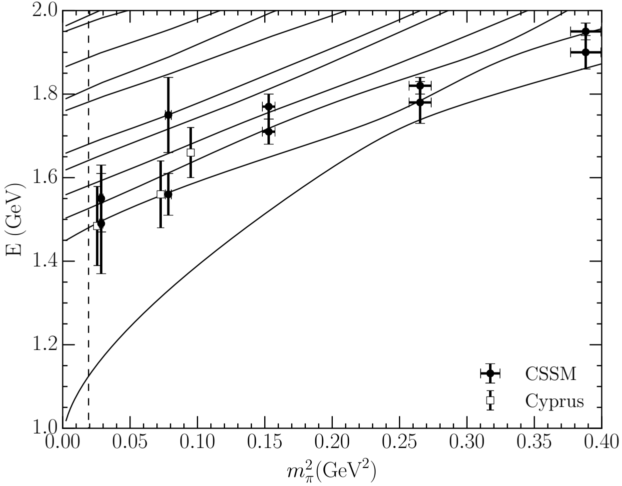

Finite-volume $L = 2$ fm energy levels for low-lying odd-parity spin-1/2 nucleons

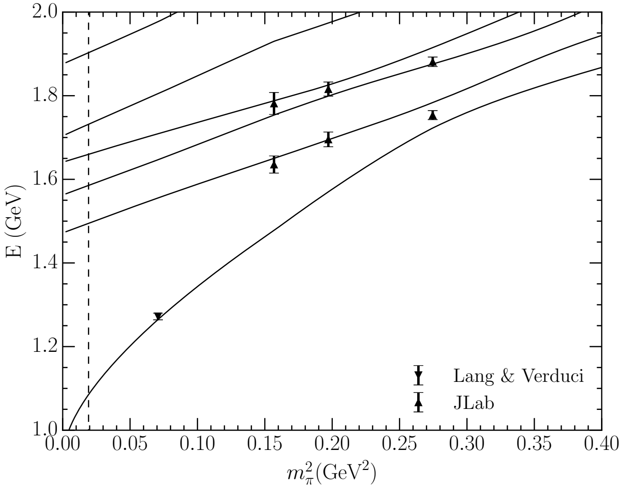

Finite-volume $L = 2$ fm energy levels for low-lying odd-parity spin-1/2 nucleons

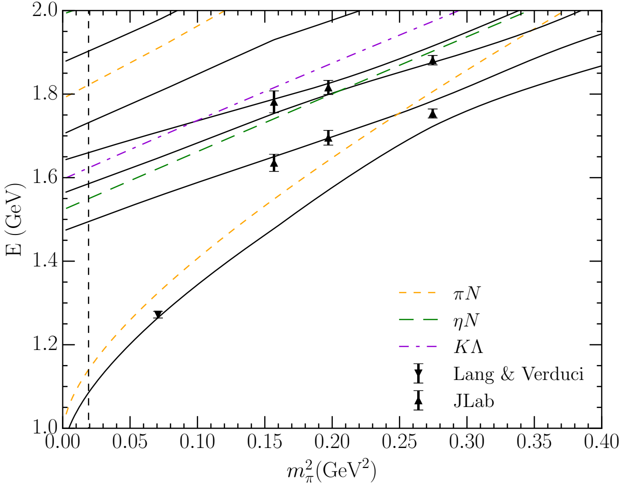

Finite Volume Eigenmode Solution

- Standard Lapack routines provide eigenmode solutions of

$$\langle\, i \,|\, H \,|\, j \,\rangle \, \langle\, j \,|\, E_\alpha \,\rangle = E_\alpha \, \langle\, i \,|\, E_\alpha \,\rangle \, .$$

- Eigenvector $\langle\, i \,|\, E_\alpha \,\rangle$ describes the composition of the eigenstate $|\, E_\alpha \,\rangle$ in terms of the basis states $|\, i \,\rangle$ with

$$|\, i \,\rangle = \,|\, B_0 \,\rangle, \quad |\, \pi N, k_0 \,\rangle, \quad |\, \pi N, k_1 \,\rangle, \quad \cdots \,|\, \eta N, k_0 \,\rangle, \quad |\, \eta N, k_1 \,\rangle, \quad \cdots \, .$$

Finite Volume Eigenmode Solution

- Standard Lapack routines provide eigenmode solutions of

$$\langle\, i \,|\, H \,|\, j \,\rangle \, \langle\, j \,|\, E_\alpha \,\rangle = E_\alpha \, \langle\, i \,|\, E_\alpha \,\rangle \,.$$

- Eigenvector $\langle\, i \,|\, E_\alpha \,\rangle$ describes the composition of the eigenstate $|\, E_\alpha \,\rangle$ in terms of the basis states $|\, i \,\rangle$ with

$$|\, i \,\rangle = |\, B_0 \,\rangle, \quad |\, \pi N, k_0 \,\rangle, \quad |\, \pi N, k_1 \,\rangle, \quad \cdots \,|\, \eta N, k_0 \,\rangle, \quad |\, \eta N, k_1 \,\rangle, \quad \cdots \,.$$

- The overlap of the bare basis state $|\, B_0 \,\rangle$ with eigenstate $|\, E_\alpha \,\rangle$,

$$\langle\, B_0 \,|\, E_\alpha \,\rangle \,,$$

  is of particular interest,

Finite Volume Eigenmode Solution

- In Hamiltonian EFT, the only localised basis state is the bare basis state.

Finite Volume Eigenmode Solution

- In Hamiltonian EFT, the only localised basis state is the bare basis state.
- Bär has highlighted how χPT provides an estimate of the direct coupling of smeared nucleon interpolating fields to a non-interacting πN (basis) state,

$$\frac{3}{16}\,\frac{1}{(f_\pi\, L)^2\, E_\pi\, L}\,\left(\frac{E_N - M_N}{E_N}\right) \sim 10^{-3}\,,$$

relative to the ground state.

O. Bar, Phys. Rev. D **92** (2015) no.7, 074504 [arXiv:1503.03649 [hep-lat]].

Finite Volume Eigenmode Solution

- In Hamiltonian EFT, the only localised basis state is the bare basis state.
- Bär has highlighted how χPT provides an estimate of the direct coupling of smeared nucleon interpolating fields to a non-interacting πN (basis) state,

$$\frac{3}{16}\,\frac{1}{(f_\pi\,L)^2\,E_\pi\,L}\left(\frac{E_N - M_N}{E_N}\right) \sim 10^{-3}\,,$$

relative to the ground state.

O. Bar, Phys. Rev. D **92** (2015) no.7, 074504 [arXiv:1503.03649 [hep-lat]].

- Conclude the smeared interpolating fields of lattice QCD are associated with the bare basis states of HEFT

$$\overline{\chi}(0)\,|\Omega\rangle \simeq |B_0\rangle\ ,$$

Finite Volume Eigenmode Solution

- In Hamiltonian EFT, the only localised basis state is the bare basis state.
- Bär has highlighted how χPT provides an estimate of the direct coupling of smeared nucleon interpolating fields to a non-interacting πN (basis) state,

$$\frac{3}{16} \frac{1}{(f_\pi\, L)^2\, E_\pi\, L} \left(\frac{E_N - M_N}{E_N} \right) \sim 10^{-3} \,,$$

  relative to the ground state.

  O. Bar, Phys. Rev. D **92** (2015) no.7, 074504 [arXiv:1503.03649 [hep-lat]].

- Conclude the smeared interpolating fields of lattice QCD are associated with the bare basis states of HEFT

$$\overline{\chi}(0)\,|\Omega\rangle \simeq |B_0\rangle \ ,$$

- Element $\langle\, B_0 \,|\, E_\alpha \,\rangle$ of the eigenvector governs the likelihood of observing $|\, E_\alpha \,\rangle$.

Finite-volume $L = 3$ fm energy levels for low-lying odd-parity spin-1/2 nucleons

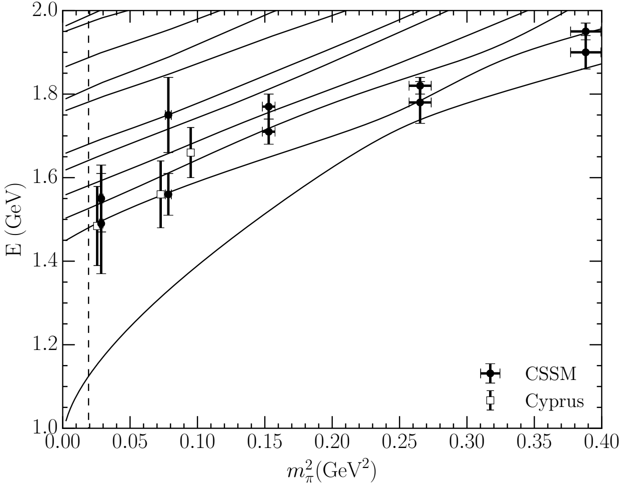

Finite-volume $L = 3$ fm energy levels for low-lying odd-parity spin-1/2 nucleons

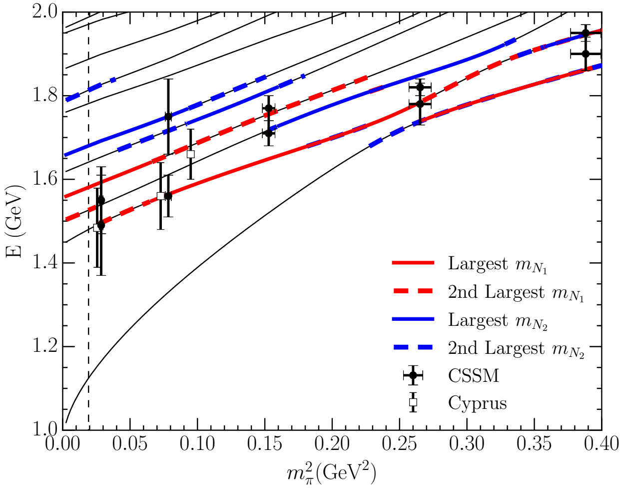

Finite-volume $L = 3$ fm energy levels for low-lying odd-parity spin-1/2 nucleons

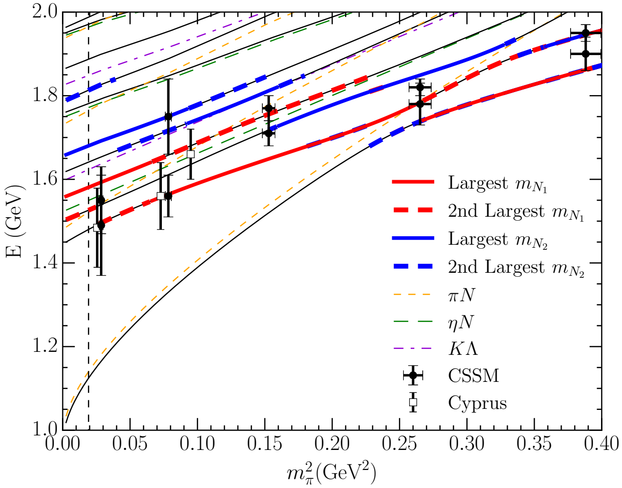

Energy eigenstate composition - 3 fm lattice

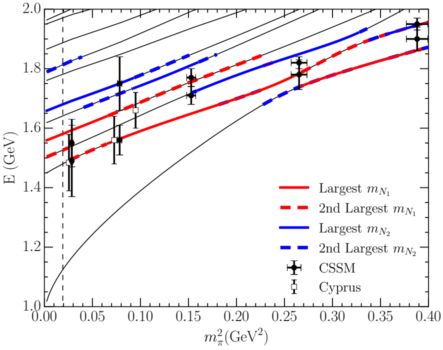

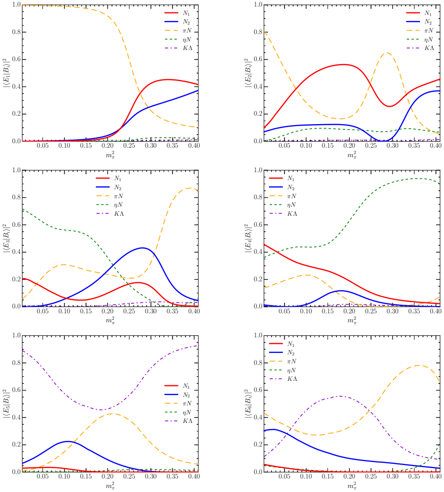

Finite-volume $L = 2$ fm energy levels for low-lying odd-parity spin-1/2 nucleons

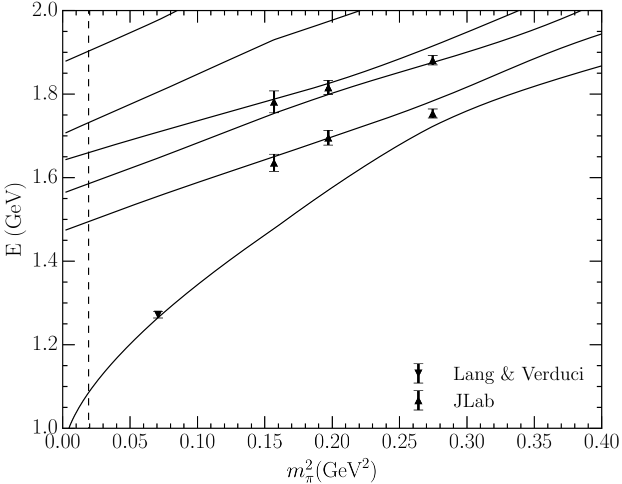

Finite-volume $L = 2$ fm energy levels for low-lying odd-parity spin-1/2 nucleons

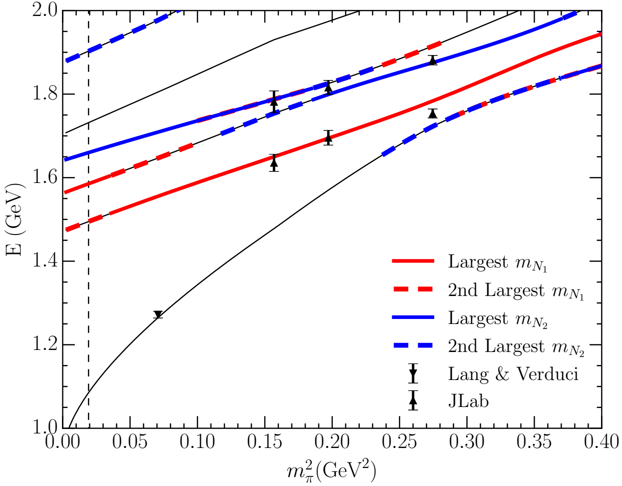

Finite-volume $L = 2$ fm energy levels for low-lying odd-parity spin-1/2 nucleons

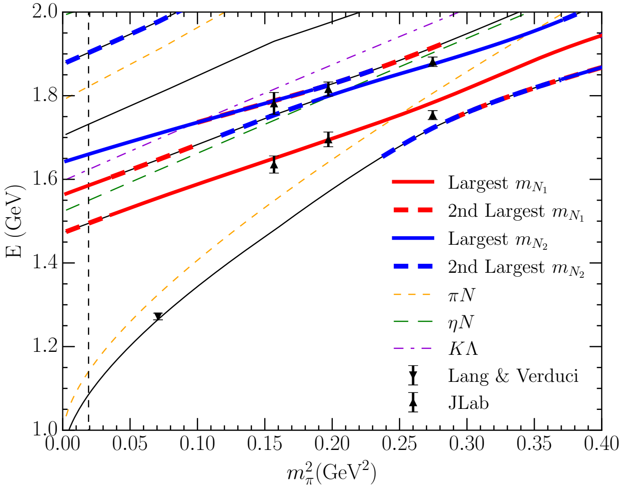

Energy eigenstate composition - 2 fm lattice

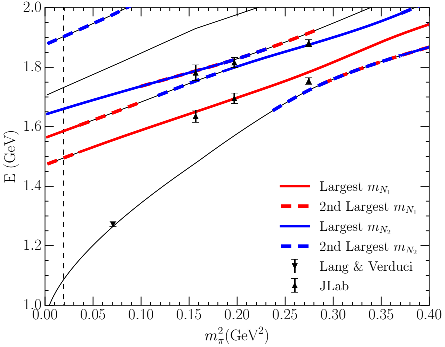

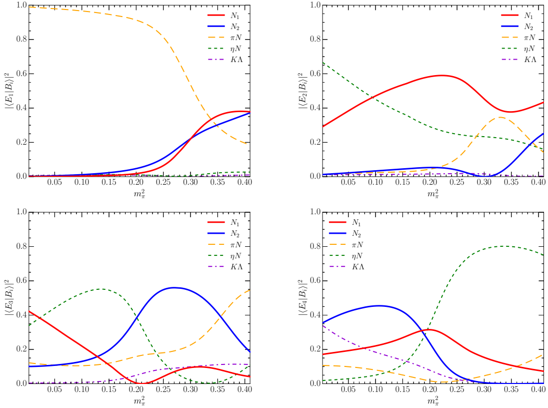

CLS Consortium finite-volume lattice energies relevant to $N1/2^-$ channel

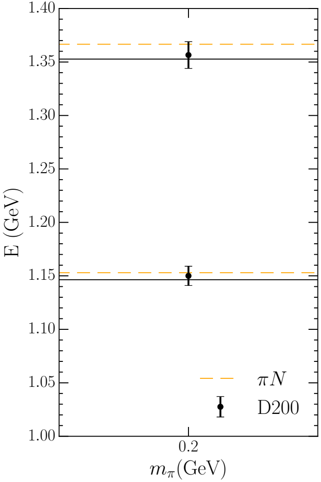

- Solid lines are HEFT energy eigenvalues.
- Bullets are lattice QCD results from

  J. Bulava, *et al.*,Nucl. Phys. B **987** (2023), 116105 [arXiv:2208.03867 [hep-lat]].

Analysis of low-lying odd-parity Λ resonances

Z. W. Liu, *et al.* [CSSM], Phys. Rev. D **95** (2017) 014506 [arXiv:1607.05856 [nucl-th]]

- Consider $\pi\Sigma$, $\bar{K}N$, $\eta\Lambda$, $K\Xi$ channels, and one bare basis state, B_0.

Analysis of low-lying odd-parity Λ resonances

Z. W. Liu, *et al.* [CSSM], Phys. Rev. D **95** (2017) 014506 [arXiv:1607.05856 [nucl-th]]

- Consider $\pi\Sigma$, $\bar{K}N$, $\eta\Lambda$, $K\Xi$ channels, and one bare basis state, B_0.
- Eight two-to-two particle couplings are considered for isospin 0 and 1

$$g^0_{\pi\Sigma,\pi\Sigma},\ g^0_{\bar{K}N,\bar{K}N},\ g^0_{\bar{K}N,\pi\Sigma},\ g^0_H,\ g^1_{\pi\Sigma,\pi\Sigma},\ g^1_{\bar{K}N,\bar{K}N},\ g^1_{\bar{K}N,\pi\Sigma},\ g^1_{\bar{K}N,\pi\Lambda},$$

Analysis of low-lying odd-parity Λ resonances

Z. W. Liu, *et al.* [CSSM], Phys. Rev. D **95** (2017) 014506 [arXiv:1607.05856 [nucl-th]]

- Consider $\pi\Sigma$, $\bar{K}N$, $\eta\Lambda$, $K\Xi$ channels, and one bare basis state, B_0.
- Eight two-to-two particle couplings are considered for isospin 0 and 1

$$g^0_{\pi\Sigma,\pi\Sigma},\ g^0_{\bar{K}N,\bar{K}N},\ g^0_{\bar{K}N,\pi\Sigma},\ g^0_{H},\ g^1_{\pi\Sigma,\pi\Sigma},\ g^1_{\bar{K}N,\bar{K}N},\ g^1_{\bar{K}N,\pi\Sigma},\ g^1_{\bar{K}N,\pi\Lambda},$$

- Five parameters describing bare to two-particle interactions are introduced

$$m_{B_0},\ g^0_{\pi\Sigma,B_0},\ g^0_{\bar{K}N,B_0},\ g^0_{\eta\Lambda,B_0},\ g^0_{K\Xi,B_0},$$

Analysis of low-lying odd-parity Λ resonances

Z. W. Liu, *et al.* [CSSM], Phys. Rev. D **95** (2017) 014506 [arXiv:1607.05856 [nucl-th]]

- Consider $\pi\Sigma$, $\bar{K}N$, $\eta\Lambda$, $K\Xi$ channels, and one bare basis state, B_0.
- Eight two-to-two particle couplings are considered for isospin 0 and 1

$$g^0_{\pi\Sigma,\pi\Sigma},\ g^0_{\bar{K}N,\bar{K}N},\ g^0_{\bar{K}N,\pi\Sigma},\ g^0_H,\ g^1_{\pi\Sigma,\pi\Sigma},\ g^1_{\bar{K}N,\bar{K}N},\ g^1_{\bar{K}N,\pi\Sigma},\ g^1_{\bar{K}N,\pi\Lambda},$$

- Five parameters describing bare to two-particle interactions are introduced

$$m_{B_0},\ g^0_{\pi\Sigma,B_0},\ g^0_{\bar{K}N,B_0},\ g^0_{\eta\Lambda,B_0},\ g^0_{K\Xi,B_0},$$

- These 13 parameters are constrained by experimental data.

Couplings and m_{B_0} Constrained by Experiment

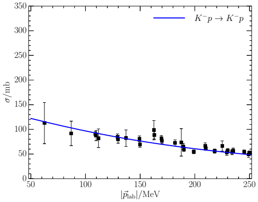

(a) $K^-p \to K^-p$

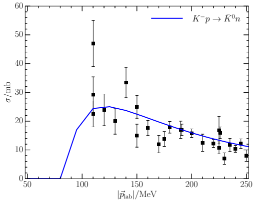

(b) $K^-p \to \bar{K}^0 n$

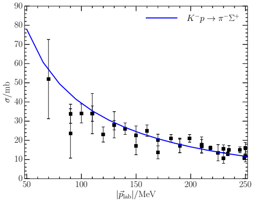

(c) $K^-p \to \pi^-\Sigma^+$

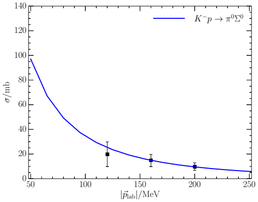

(d) $K^-p \to \pi^0\Sigma^0$

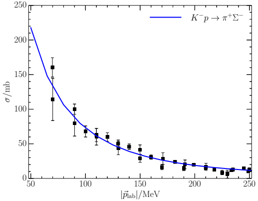

(e) $K^-p \to \pi^+\Sigma^-$

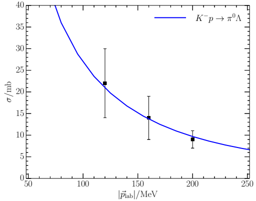

(f) $K^-p \to \pi^0\Lambda$

Finite Volume Λ Spectrum for $L = 3$ fm

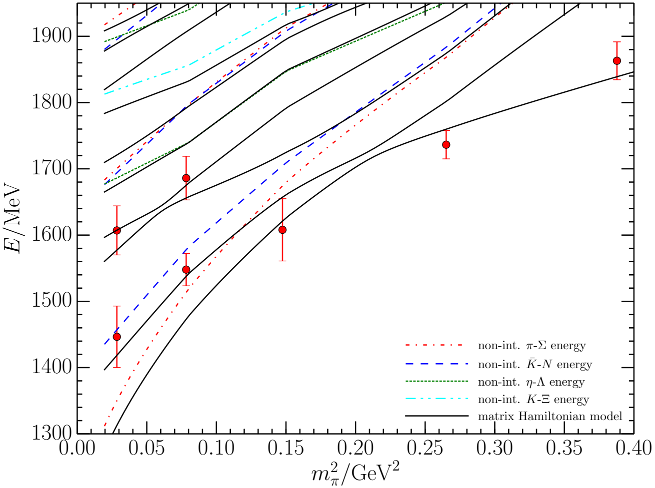

Finite Volume Λ Spectrum for $L = 3$ fm

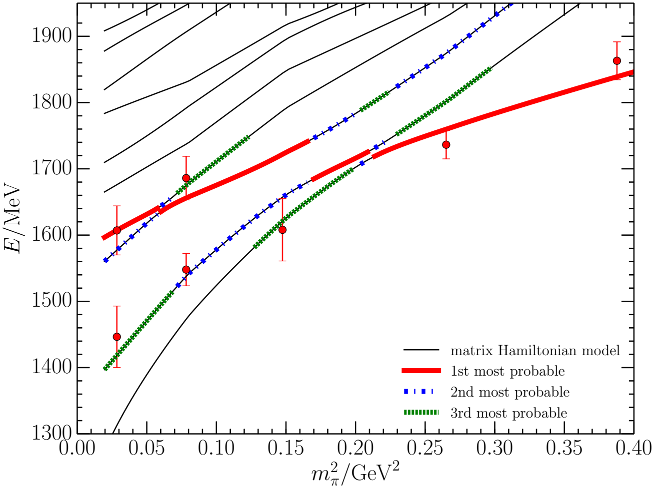

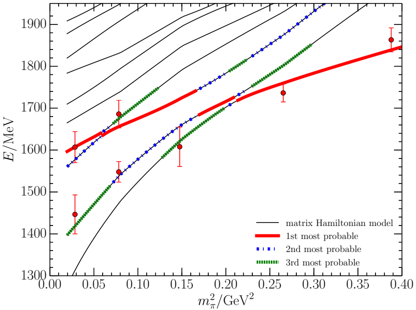

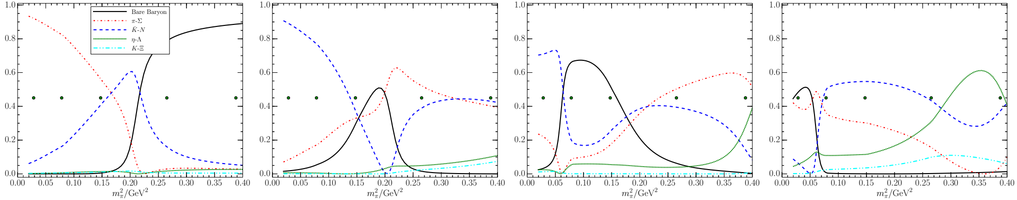

(a) State 1 (b) State 2 (c) State 3 (d) State 4

Where is the Roper resonance?

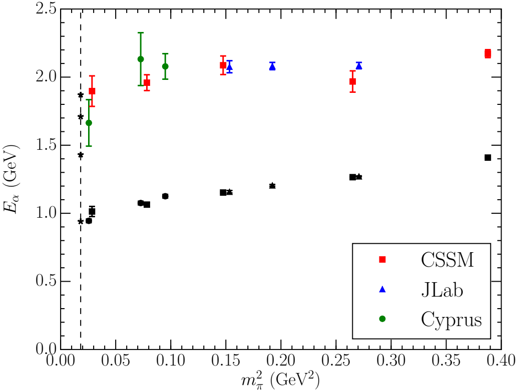

- Cyprus: C. Alexandrou, *et al.* (AMIAS), Phys. Rev. D **91**, 014506 (2015) arXiv:1411.6765 [hep-lat]
- CSSM: Z. W. Liu, *et al.* [CSSM], Phys. Rev. D **95**, 034034 (2017) arXiv:1607.04536 [nucl-th]
- JLab: R. G. Edwards, *et al.* [HSC] Phys. Rev. D **84**, 074508 (2011) [arXiv:1104.5152 [hep-ph]].

Search for low-lying lattice QCD eigenstates in the Roper regime

A. L. Kiratidis, *et al.*, [CSSM] Phys. Rev. D **95**, no. 7, 074507 (2017) [arXiv:1608.03051 [hep-lat]].

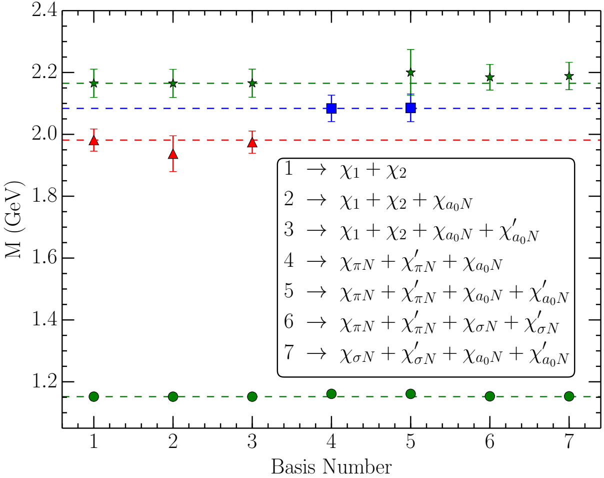

Have we seen the $2s$ excitation of the quark model?

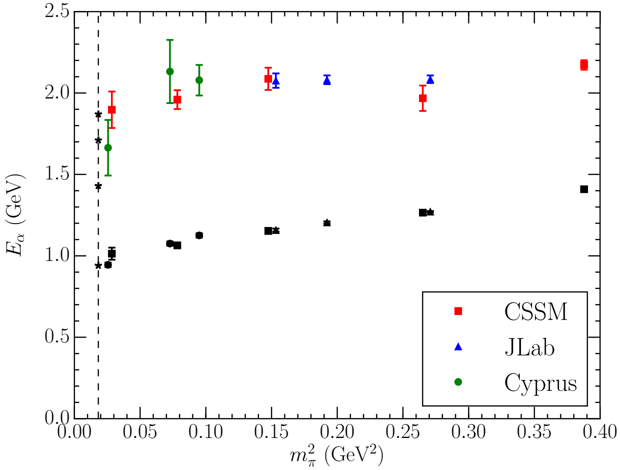

Landau-Gauge Wave functions from the Lattice

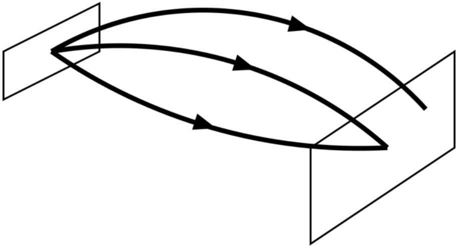

- Measure the *overlap* of the annihilation operator with the state as a function of the quark positions.

d-quark probability density in ground state proton [CSSM]

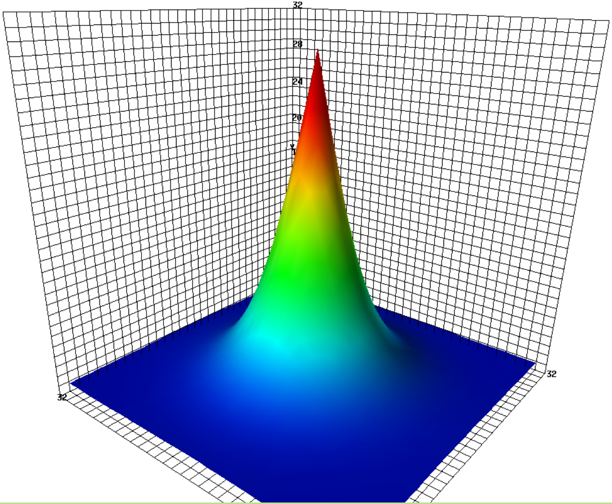

d-quark probability density in 1st excited state of proton [CSSM]

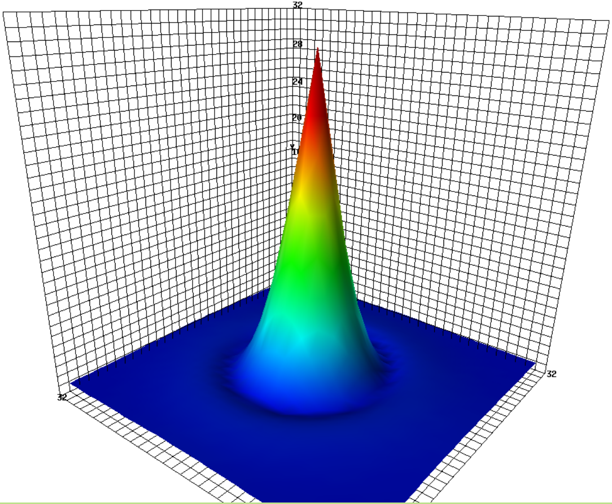

d-quark probability density in $N = 3$ excited state of proton [CSSM]

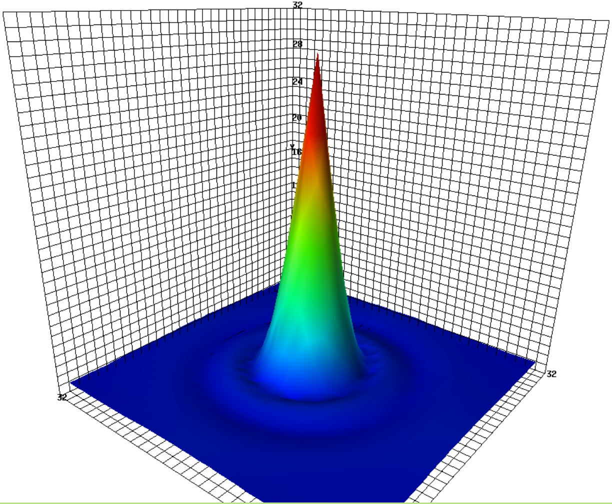

Comparison with the Simple Quark Model [CSSM]

D. S. Roberts, W. Kamleh and D. B. Leinweber, Phys. Lett. B **725**, 164 (2013) [arXiv:1304.0325 [hep-lat]].

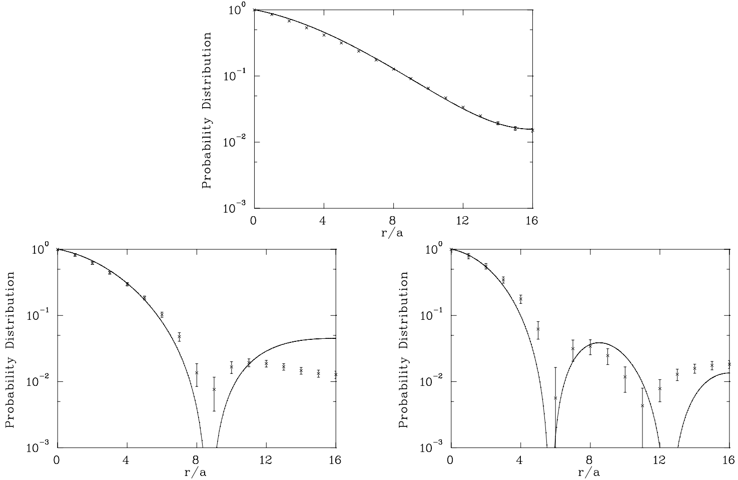

First positive-parity excitation: Charge Radii

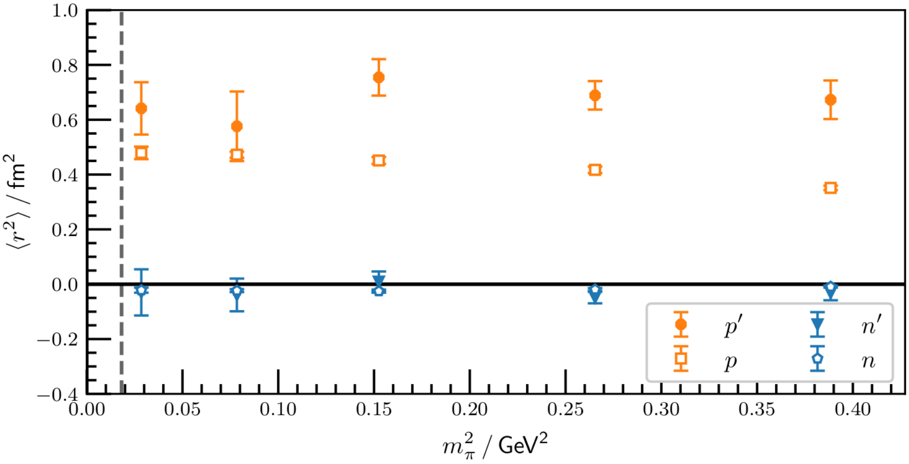

F. M. Stokes, W. Kamleh, DBL, Phys. Rev. D **102** (2020) 014507 [arXiv:1907.00177 [hep-lat]].

First positive-parity excitation: Magnetic moments

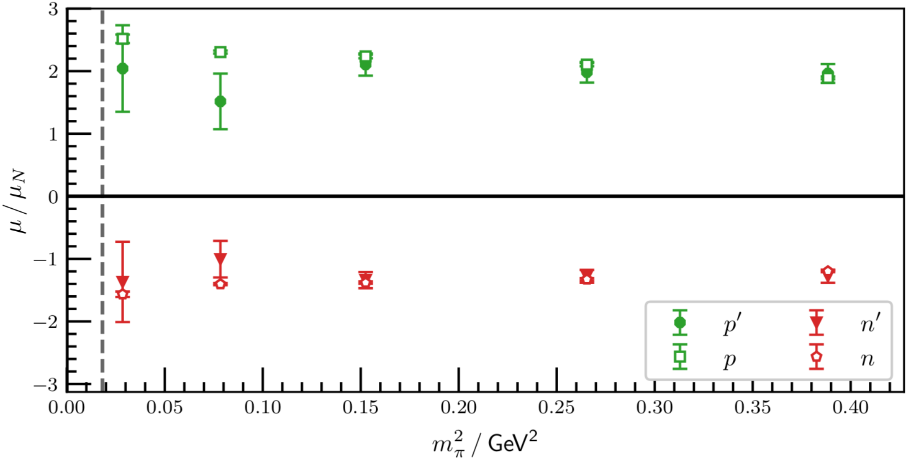

F. M. Stokes, W. Kamleh, DBL, Phys. Rev. D **102** (2020) 014507 [arXiv:1907.00177 [hep-lat]].

The $2s$ excitation of the nucleon sits at 1.9 GeV

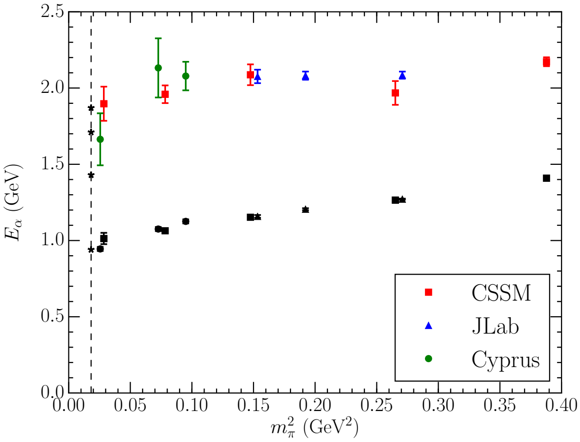

The $2s$ excitation of the nucleon sits at 1.9 GeV

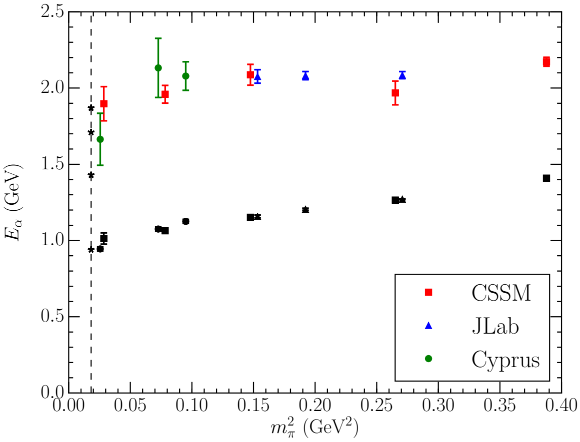

- Quark model states are basis states that mix with meson-baryon multiparticle states.

The $2s$ excitation of the nucleon sits at 1.9 GeV

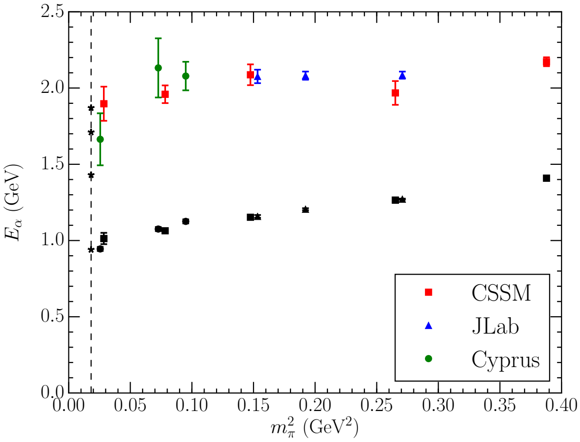

- Quark model states are basis states that mix with meson-baryon multiparticle states.
- Anticipate the $2s$ excitation is associated with
  - $N1/2^+(1880)$ observed in photoproduction.
  - $N1/2^+(1710)$ only 170 MeV away.

The $2s$ excitation of the nucleon sits at 1.9 GeV

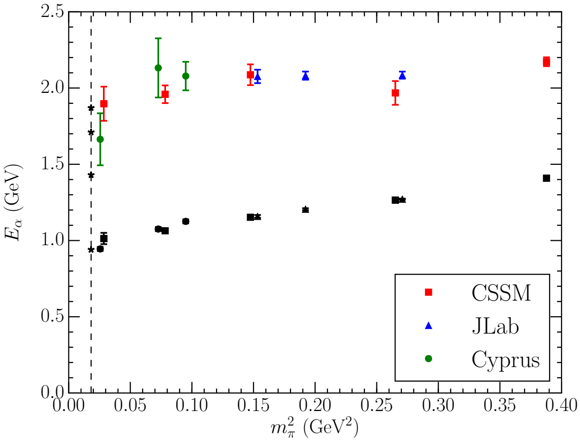

- Quark model states are basis states that mix with meson-baryon multiparticle states.
- Anticipate the $2s$ excitation is associated with
  - $N1/2^+(1880)$ observed in photoproduction.
  - $N1/2^+(1710)$ only 170 MeV away.
- What about the Roper resonance?

Positive-parity Nucleon Spectrum: Bare Basis State with $m_0 = 1.7$ GeV

- Consider πN, $\pi\Delta$ and σN channels, dressing a bare basis state.
- Fit to phase shift and inelasticity. (dashed blue curve)

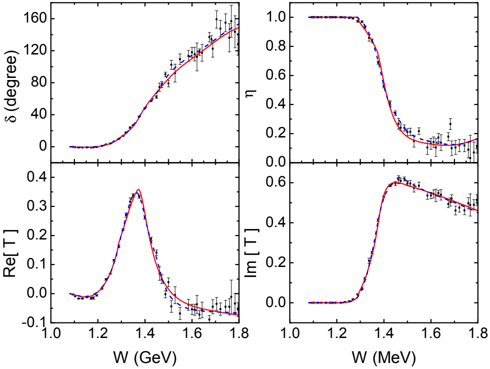

- Fit yields two poles in the region of the PDG estimate $1365 \pm 15 - i\,95 \pm 15$ MeV.

1.7 GeV Bare Basis State: Hamiltonian Model N' Spectrum

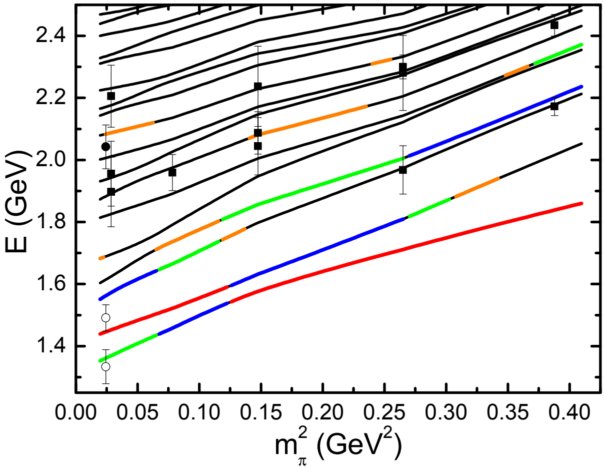

Positive-parity Nucleon Spectrum: Bare Basis State with $m_0 = 2.0$ GeV

J. j. Wu, *et al.* [CSSM], arXiv:1703.10715 [nucl-th]

- Consider πN, $\pi\Delta$ and σN channels, dressing a bare basis state.
- Fit to phase shift and inelasticity. (red curve)

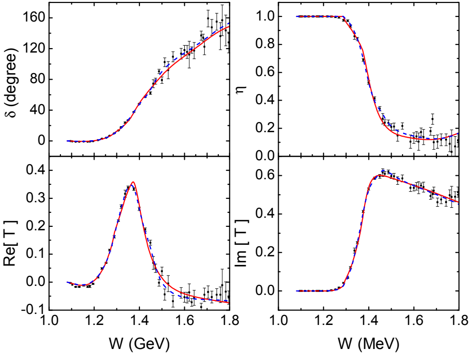

- Fit yields a pole in the regime of the PDG estimate $1365 \pm 15 - i\,95 \pm 15$ MeV.

2.0 GeV Bare Basis State: Hamiltonian Model N' Spectrum

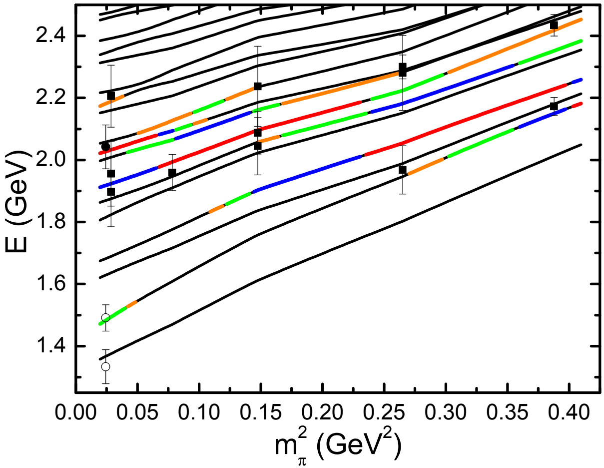

2.0 GeV Bare Basis State: Hamiltonian Model N' Spectrum

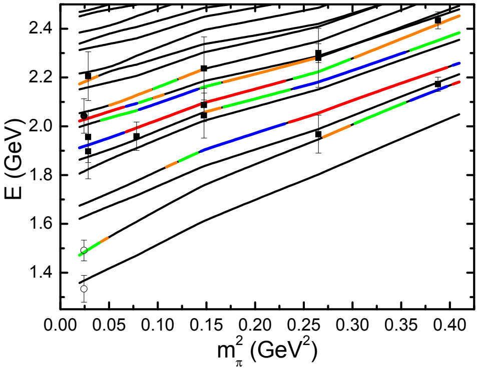

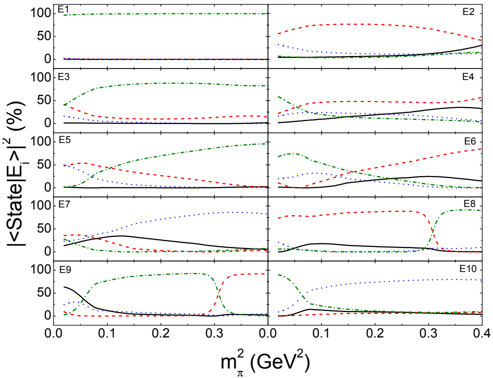

πN, $\pi\Delta$ and σN channels, dressing a bare state.

C. B. Lang, L. Leskovec, M. Padmanath and S. Prelovsek, Phys. Rev. D **95**, no. 1, 014510 (2017) [arXiv:1610.01422 [hep-lat]].

Two different descriptions of the Roper resonance

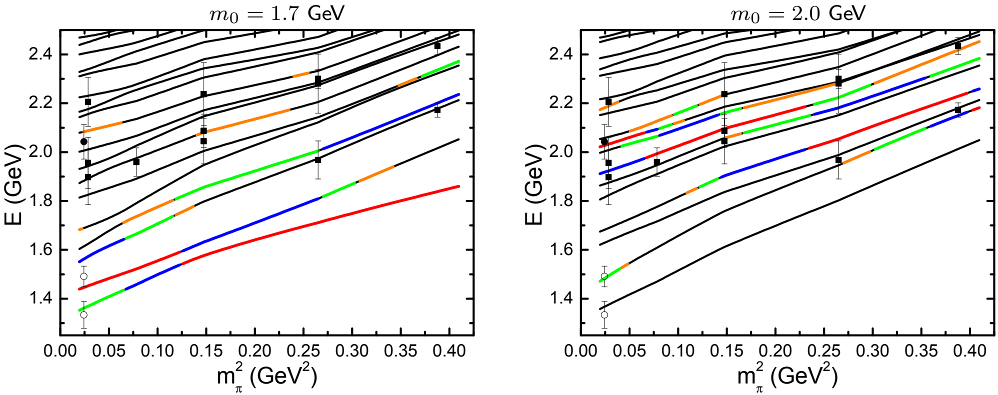

(left) Meson dressings of a quark-model like core.

(right) Resonance generated by strong rescattering in meson-baryon channels.

Score Card

Criteria	$m_0 = 1.7$ GeV	$m_0 = 2.0$ GeV
Describes experimental data well.		

Score Card

Criteria	$m_0 = 1.7$ GeV	$m_0 = 2.0$ GeV
Describes experimental data well.	✔	✔

Score Card

Criteria	$m_0 = 1.7$ GeV	$m_0 = 2.0$ GeV
Describes experimental data well.	✔	✔
Produces poles in accord with PDG.		

Score Card

Criteria	$m_0 = 1.7$ GeV	$m_0 = 2.0$ GeV
Describes experimental data well.	✔	✔
Produces poles in accord with PDG.	✔	✔

Score Card

Criteria	$m_0 = 1.7$ GeV	$m_0 = 2.0$ GeV
Describes experimental data well.	✔	✔
Produces poles in accord with PDG.	✔	✔
1st lattice scattering state created via σN interpolator has dominant $\langle \sigma N \mid E_1 \rangle$ in HEFT.		

Score Card

Criteria	$m_0 = 1.7$ GeV	$m_0 = 2.0$ GeV
Describes experimental data well.	✔	✔
Produces poles in accord with PDG.	✔	✔
1st lattice scattering state created via σN interpolator has dominant $\langle \sigma N \mid E_1 \rangle$ in HEFT.	✔	✔

Score Card

Criteria	$m_0 = 1.7$ GeV	$m_0 = 2.0$ GeV
Describes experimental data well.	✔	✔
Produces poles in accord with PDG.	✔	✔
1st lattice scattering state created via σN interpolator has dominant $\langle \sigma N \mid E_1 \rangle$ in HEFT.	✔	✔
2nd lattice scattering state created via πN interpolator has dominant $\langle \pi N \mid E_2 \rangle$ in HEFT.		

Score Card

Criteria	$m_0 = 1.7$ GeV	$m_0 = 2.0$ GeV
Describes experimental data well.	✔	✔
Produces poles in accord with PDG.	✔	✔
1st lattice scattering state created via σN interpolator has dominant $\langle\, \sigma N \,|\, E_1 \,\rangle$ in HEFT.	✔	✔
2nd lattice scattering state created via πN interpolator has dominant $\langle\, \pi N \,|\, E_2 \,\rangle$ in HEFT.	✗	✔

Score Card

Criteria	$m_0 = 1.7$ GeV	$m_0 = 2.0$ GeV
Describes experimental data well.	✔	✔
Produces poles in accord with PDG.	✔	✔
1st lattice scattering state created via σN interpolator has dominant $\langle \sigma N \mid E_1 \rangle$ in HEFT.	✔	✔
2nd lattice scattering state created via πN interpolator has dominant $\langle \pi N \mid E_2 \rangle$ in HEFT.	✗	✔
L-QCD states excited with 3-quark ops. are associated with HEFT states with large $\langle B_0 \mid E_\alpha \rangle$.		

Score Card

Criteria	$m_0 = 1.7$ GeV	$m_0 = 2.0$ GeV
Describes experimental data well.	✔	✔
Produces poles in accord with PDG.	✔	✔
1st lattice scattering state created via σN interpolator has dominant $\langle\, \sigma N \,|\, E_1 \,\rangle$ in HEFT.	✔	✔
2nd lattice scattering state created via πN interpolator has dominant $\langle\, \pi N \,|\, E_2 \,\rangle$ in HEFT.	✗	✔
L-QCD states excited with 3-quark ops. are associated with HEFT states with large $\langle\, B_0 \,|\, E_\alpha \,\rangle$.	✗	✔

Score Card

Criteria	$m_0 = 1.7$ GeV	$m_0 = 2.0$ GeV
Describes experimental data well.	✔	✔
Produces poles in accord with PDG.	✔	✔
1st lattice scattering state created via σN interpolator has dominant $\langle \sigma N \mid E_1 \rangle$ in HEFT.	✔	✔
2nd lattice scattering state created via πN interpolator has dominant $\langle \pi N \mid E_2 \rangle$ in HEFT.	✗	✔
L-QCD states excited with 3-quark ops. are associated with HEFT states with large $\langle B_0 \mid E_\alpha \rangle$.	✗	✔
HEFT predicts three-quark states that exist in lattice QCD.		

Score Card

Criteria	$m_0 = 1.7$ GeV	$m_0 = 2.0$ GeV
Describes experimental data well.	✔	✔
Produces poles in accord with PDG.	✔	✔
1st lattice scattering state created via σN interpolator has dominant $\langle\, \sigma N \,\vert\, E_1 \,\rangle$ in HEFT.	✔	✔
2nd lattice scattering state created via πN interpolator has dominant $\langle\, \pi N \,\vert\, E_2 \,\rangle$ in HEFT.	✗	✔
L-QCD states excited with 3-quark ops. are associated with HEFT states with large $\langle\, B_0 \,\vert\, E_\alpha \,\rangle$.	✗	✔
HEFT predicts three-quark states that exist in lattice QCD.	✗	✔

Two different descriptions of the Roper resonance

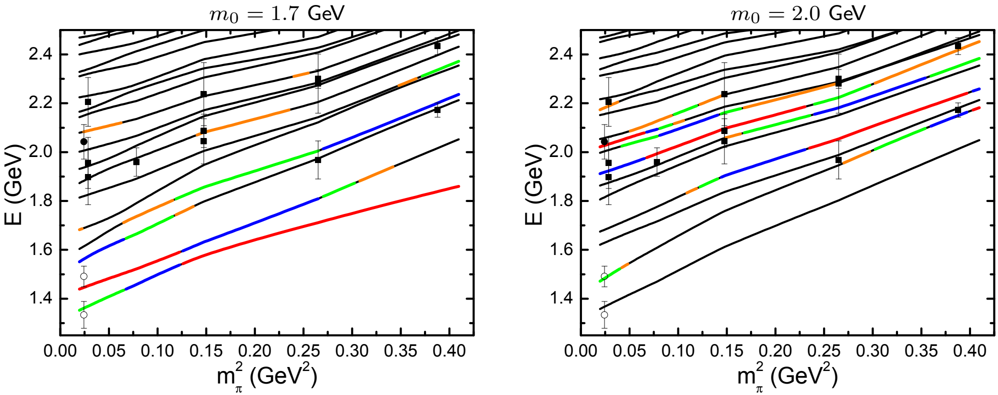

(left) Meson dressings of a quark-model like core.

(right) Resonance generated by strong rescattering in meson-baryon channels.

Conclusion

- The Roper resonance is not associated with a low-lying three-quark core.

Conclusion

- The Roper resonance is not associated with a low-lying three-quark core.
- The Roper resonance is generated by strong rescattering in meson-baryon channels.

Conclusion

- The Roper resonance is not associated with a low-lying three-quark core.
- The Roper resonance is generated by strong rescattering in meson-baryon channels.

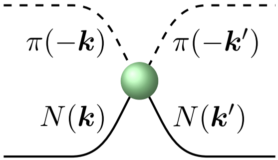

Conclusion

- The Roper resonance is not associated with a low-lying three-quark core.
- The Roper resonance is generated by strong rescattering in meson-baryon channels.

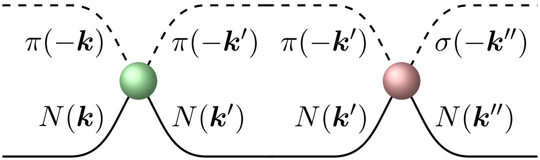

Conclusion

- The Roper resonance is not associated with a low-lying three-quark core.
- The Roper resonance is generated by strong rescattering in meson-baryon channels.

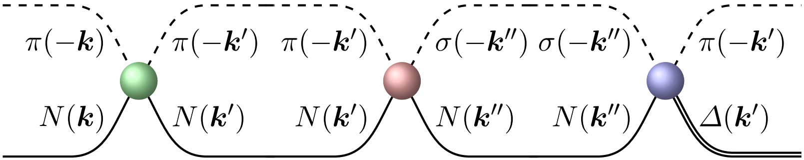

Conclusion

- The Roper resonance is not associated with a low-lying three-quark core.
- The Roper resonance is generated by strong rescattering in meson-baryon channels.

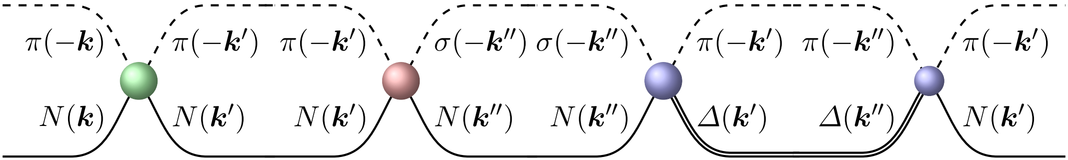

Conclusion

- The Roper resonance is not associated with a low-lying three-quark core.
- The Roper resonance is generated by strong rescattering in meson-baryon channels.

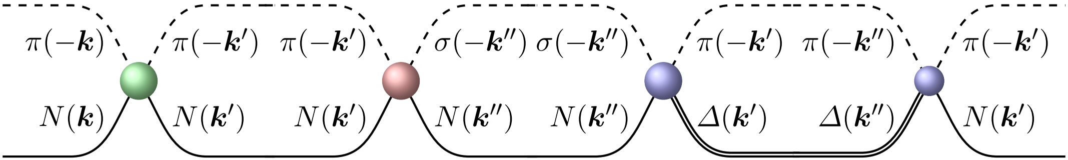

- The $2s$ excitation of the nucleon is dressed to lie at ~ 1.9 GeV

Δ-baryon spectrum from lattice QCD

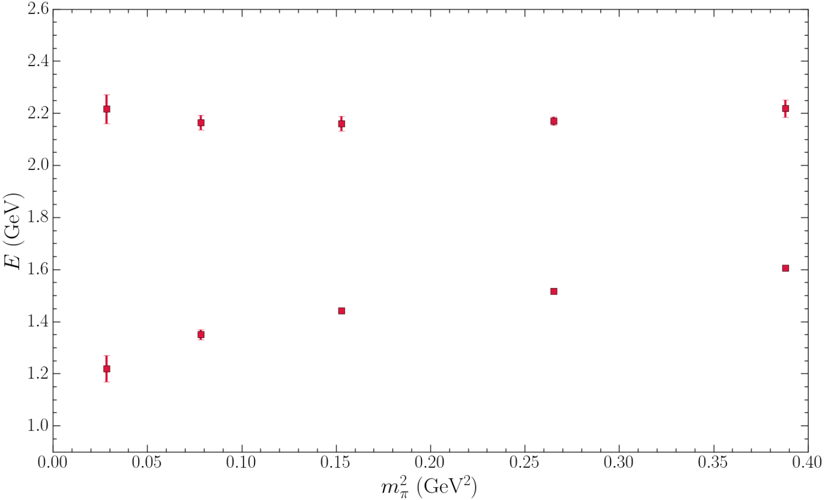

Δ-baryon spectrum from lattice QCD

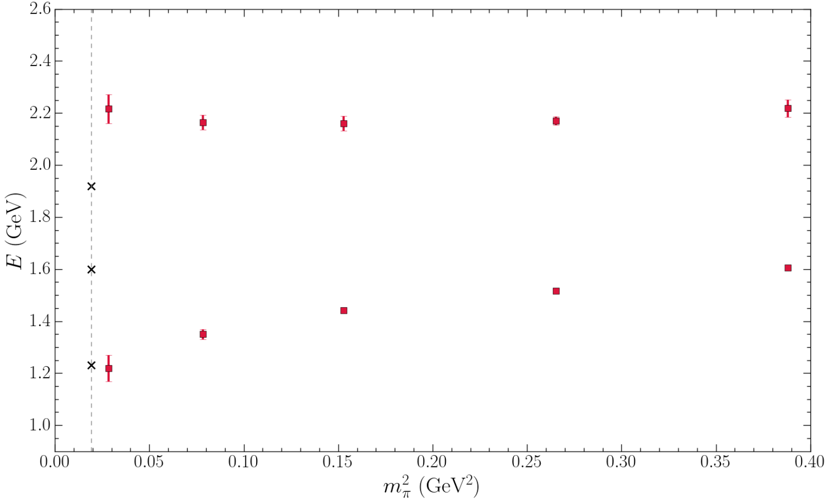

Missing Baryon Resonances

- Many resonances predicted by the constituent quark model (CQM) below 2 GeV are not seen.

Missing Baryon Resonances

- Many resonances predicted by the constituent quark model (CQM) below 2 GeV are not seen.
- Now know the CQM should have been tuned to a $2s$ resonance at ~ 1900 MeV.
  - Further excitations are at energies exceeding 2 GeV.

Missing Baryon Resonances

- Many resonances predicted by the constituent quark model (CQM) below 2 GeV are not seen.
- Now know the CQM should have been tuned to a $2s$ resonance at ~ 1900 MeV.
  - Further excitations are at energies exceeding 2 GeV.
- Provides a new resolution of the missing baryon resonance problem.

Nucleon and Delta Resonance Predistions from the Quark Model

S. Capstick and W. Roberts, Phys. Rev. D **47** (1993), 1994-2010.

Model state	$\lvert A_{N\pi}\rvert$ (MeV$^{\frac{1}{2}}$)	$N\pi$ state assignment	Rating	$\sqrt{\Gamma_{tot}}(BR)_{N\pi}$ (MeV$^{\frac{1}{2}}$)
$[N\frac{1}{2}^+]_2(1540)$	$20.3^{+0.8}_{-0.9}$	$N\frac{1}{2}^+(1440)$	****	19.9±3.0
$[N\frac{1}{2}^+]_3(1770)$	4.2 ± 0.1	$N\frac{1}{2}^+(1710)$	***	4.7±1.2
$[N\frac{1}{2}^+]_4(1880)$	$2.7^{+0.6}_{-0.9}$			
$[N\frac{1}{2}^+]_5(1975)$	$2.0^{+0.2}_{-0.3}$			
$[\Delta\frac{3}{2}^+]_1(1230)$	10.4 ± 0.1	$\Delta\frac{3}{2}^+(1232)$	****	10.7±0.3
$[\Delta\frac{3}{2}^+]_2(1795)$	8.7 ± 0.2	$\Delta\frac{3}{2}^+(1600)$	**	7.6±2.3
$[\Delta\frac{3}{2}^+]_3(1915)$	4.2 ± 0.3	$\Delta\frac{3}{2}^+(1920)$	***	7.7±2.3
$[\Delta\frac{3}{2}^+]_4(1985)$	$3.3^{+0.8}_{-1.1}$			

Nucleon and Delta Resonance Predistions from the Quark Model

S. Capstick and W. Roberts, Phys. Rev. D **47** (1993), 1994-2010.

Model state	$\|A_{N\pi}\|$ (MeV$^{\frac{1}{2}}$)	$N\pi$ state assignment	Rating	$\sqrt{\Gamma_{tot}}(\mathrm{BR})_{N\pi}$ (MeV$^{\frac{1}{2}}$)
$[N\frac{1}{2}^+]_2(1540)$	$20.3^{+0.8}_{-0.9}$	$N\frac{1}{2}^+(1440)$	****	19.9±3.0
$[N\frac{1}{2}^+]_3(1770)$	4.2 ± 0.1	$N\frac{1}{2}^+(1710)$	***	4.7±1.2
$[N\frac{1}{2}^+]_4(1880)$	$2.7^{+0.6}_{-0.9}$			
$[N\frac{1}{2}^+]_5(1975)$	$2.0^{+0.2}_{-0.3}$			
$[\Delta\frac{3}{2}^+]_1(1230)$	10.4 ± 0.1	$\Delta\frac{3}{2}^+(1232)$	****	10.7±0.3
$[\Delta\frac{3}{2}^+]_2(1795)$	8.7 ± 0.2	$\Delta\frac{3}{2}^+(1600)$	**	7.6±2.3
$[\Delta\frac{3}{2}^+]_3(1915)$	4.2 ± 0.3	$\Delta\frac{3}{2}^+(1920)$	***	7.7±2.3
$[\Delta\frac{3}{2}^+]_4(1985)$	$3.3^{+0.8}_{-1.1}$			

Nucleon and Delta Resonance Predistions from the Quark Model

S. Capstick and W. Roberts, Phys. Rev. D **47** (1993), 1994-2010.

Model state	$\lvert A_{N\pi} \rvert$ (MeV$^{\frac{1}{2}}$)	$N\pi$ state assignment	Rating	$\sqrt{\Gamma_{\text{tot}}}(\text{BR})_{N\pi}$ (MeV$^{\frac{1}{2}}$)
$[N\frac{1}{2}^+]_2$(~~1540~~) 1900	$20.3^{+0.8}_{-0.9}$	$N\frac{1}{2}^+(1440)$	****	19.9±3.0
$[N\frac{1}{2}^+]_3$(~~1770~~) 2600	4.2 ± 0.1	$N\frac{1}{2}^+(1710)$	***	4.7±1.2
$[N\frac{1}{2}^+]_4(1880)$	$2.7^{+0.6}_{-0.9}$			
$[N\frac{1}{2}^+]_5(1975)$	$2.0^{+0.2}_{-0.3}$			
$[\Delta\frac{3}{2}^+]_1(1230)$	10.4 ± 0.1	$\Delta\frac{3}{2}^+(1232)$	****	10.7±0.3
$[\Delta\frac{3}{2}^+]_2(1795)$	8.7 ± 0.2	$\Delta\frac{3}{2}^+(1600)$	**	7.6±2.3
$[\Delta\frac{3}{2}^+]_3(1915)$	4.2 ± 0.3	$\Delta\frac{3}{2}^+(1920)$	***	7.7±2.3
$[\Delta\frac{3}{2}^+]_4(1985)$	$3.3^{+0.8}_{-1.1}$			

Nucleon and Delta Resonance Predistions from the Quark Model

S. Capstick and W. Roberts, Phys. Rev. D **47** (1993), 1994-2010.

Model state	$\lvert A_{N\pi} \rvert$ ($\mathrm{MeV}^{\frac{1}{2}}$)	$N\pi$ state assignment	Rating	$\sqrt{\Gamma_{\mathrm{tot}}}(\mathrm{BR})_{N\pi}$ ($\mathrm{MeV}^{\frac{1}{2}}$)
$[N\frac{1}{2}^{+}]_2(1540)$ 1900	$20.3^{+0.8}_{-0.9}$	$N\frac{1}{2}^{+}(1440)$	****	19.9±3.0
$[N\frac{1}{2}^{+}]_3(1770)$ 2600	4.2 ± 0.1	$N\frac{1}{2}^{+}(1710)$	***	4.7±1.2
$[N\frac{1}{2}^{+}]_4(1880)$	$2.7^{+0.6}_{-0.9}$			
$[N\frac{1}{2}^{+}]_5(1975)$	$2.0^{+0.2}_{-0.3}$			
$[\Delta\frac{3}{2}^{+}]_1(1230)$	10.4 ± 0.1	$\Delta\frac{3}{2}^{+}(1232)$	****	10.7±0.3
$[\Delta\frac{3}{2}^{+}]_2(1795)$ 2200	8.7 ± 0.2	$\Delta\frac{3}{2}^{+}(1600)$	**	7.6±2.3
$[\Delta\frac{3}{2}^{+}]_3(1915)$	4.2 ± 0.3	$\Delta\frac{3}{2}^{+}(1920)$	***	7.7±2.3
$[\Delta\frac{3}{2}^{+}]_4(1985)$	$3.3^{+0.8}_{-1.1}$			

Conclusions

- Hamiltonian Effective Field Theory (HEFT)
  - Connects infinite-volume scattering observables to finite-volume Lattice QCD.

Conclusions

- Hamiltonian Effective Field Theory (HEFT)
  - Connects infinite-volume scattering observables to finite-volume Lattice QCD.
  - Connects lattice results at different quark masses within a single formalism.

Conclusions

- Hamiltonian Effective Field Theory (HEFT)
  - Connects infinite-volume scattering observables to finite-volume Lattice QCD.
  - Connects lattice results at different quark masses within a single formalism.
  - Provides insight into the composition of energy eigenstates.
  - Facilitates an understanding of lattice QCD results.

Conclusions

- Hamiltonian Effective Field Theory (HEFT)
  - Connects infinite-volume scattering observables to finite-volume Lattice QCD.
  - Connects lattice results at different quark masses within a single formalism.
  - Provides insight into the composition of energy eigenstates.
  - Facilitates an understanding of lattice QCD results.
  - With lattice QCD constraints, HEFT provides new insight into resonance structure.

Conclusions

- Hamiltonian Effective Field Theory (HEFT)
  - Connects infinite-volume scattering observables to finite-volume Lattice QCD.
  - Connects lattice results at different quark masses within a single formalism.
  - Provides insight into the composition of energy eigenstates.
  - Facilitates an understanding of lattice QCD results.
  - With lattice QCD constraints, HEFT provides new insight into resonance structure.
- Δ Resonance: illustrate Lüscher constraints and the role of lattice QCD constraints.

Conclusions

- Hamiltonian Effective Field Theory (HEFT)
  - Connects infinite-volume scattering observables to finite-volume Lattice QCD.
  - Connects lattice results at different quark masses within a single formalism.
  - Provides insight into the composition of energy eigenstates.
  - Facilitates an understanding of lattice QCD results.
  - With lattice QCD constraints, HEFT provides new insight into resonance structure.
- Δ Resonance: illustrate Lüscher constraints and the role of lattice QCD constraints.
- Odd-parity $N^*(1535)$ and $N^*(1650)$ Resonances:
  - Knowledge of eigenstate composition can be used to understand the states observed.
  - Dominated by a quark-core bare state dressed by meson degrees of freedom.

Conclusions

- Hamiltonian Effective Field Theory (HEFT)
  - Connects infinite-volume scattering observables to finite-volume Lattice QCD.
  - Connects lattice results at different quark masses within a single formalism.
  - Provides insight into the composition of energy eigenstates.
  - Facilitates an understanding of lattice QCD results.
  - With lattice QCD constraints, HEFT provides new insight into resonance structure.
- Δ Resonance: illustrate Lüscher constraints and the role of lattice QCD constraints.
- Odd-parity $N^*(1535)$ and $N^*(1650)$ Resonances:
  - Knowledge of eigenstate composition can be used to understand the states observed.
  - Dominated by a quark-core bare state dressed by meson degrees of freedom.
- Roper $N(1440)$ Resonance: Arises from dynamical coupled-channel effects.
  - Lattice QCD results constrain the HEFT description of experimental data.
  - State composition matches when the $2s$ excitation of the quark model sits at ~ 2 GeV.

The spectrum of quark-model-like states is relatively simple

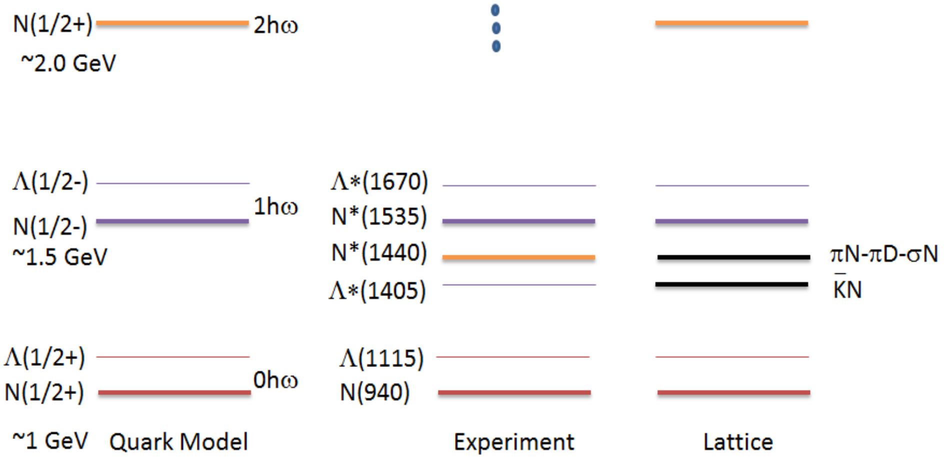

HEFT Extensions

- Formalism for partial-wave mixing in HEFT has been developed in Y. Li, J. J. Wu, C. D. Abell, D. B. L. and A. W. Thomas. Phys. Rev. D **101**, no.11, 114501 (2020) [arXiv:1910.04973 [hep-lat]]

- And extended to moving and elongated finite-volumes in Y. Li, J. J. Wu, D. B. L. and A. W. Thomas Phys. Rev. D **103** no.9, 094518 (2021) [arXiv:2103.12260 [hep-lat]].

Evidence the $2s$ state is associated with the $N1/2^+(1710)$ and $N1/2^+(1880)$

- The $N1/2^+(1880)$ was observed in photoproduction while missed in πN scattering.

Evidence the $2s$ state is associated with the $N1/2^+(1710)$ and $N1/2^+(1880)$

- The $N1/2^+(1880)$ was observed in photoproduction while missed in πN scattering.
- The $N1/2^+(1710)$ has a small width of 140 MeV and perhaps as small as 80 MeV.

Evidence the $2s$ state is associated with the $N1/2^+(1710)$ and $N1/2^+(1880)$

- The $N1/2^+(1880)$ was observed in photoproduction while missed in πN scattering.
- The $N1/2^+(1710)$ has a small width of 140 MeV and perhaps as small as 80 MeV.
- Both suggest the $2s$ excitation on the lattice may be insensitive to modifications of the meson dressings.

Evidence the $2s$ state is associated with the $N1/2^+(1710)$ and $N1/2^+(1880)$

- The $N1/2^+(1880)$ was observed in photoproduction while missed in πN scattering.
- The $N1/2^+(1710)$ has a small width of 140 MeV and perhaps as small as 80 MeV.
- Both suggest the $2s$ excitation on the lattice may be insensitive to modifications of the meson dressings.
- Consider a quenched QCD simulation with matched lattice spacing and quark masses.

Evidence the $2s$ state is associated with the $N1/2^+(1710)$ and $N1/2^+(1880)$

- The $N1/2^+(1880)$ was observed in photoproduction while missed in πN scattering.
- The $N1/2^+(1710)$ has a small width of 140 MeV and perhaps as small as 80 MeV.
- Both suggest the $2s$ excitation on the lattice may be insensitive to modifications of the meson dressings.
- Consider a quenched QCD simulation with matched lattice spacing and quark masses.
  - Couplings to meson dressings are suppressed.

Evidence the $2s$ state is associated with the $N1/2^+(1710)$ and $N1/2^+(1880)$

- The $N1/2^+(1880)$ was observed in photoproduction while missed in πN scattering.
- The $N1/2^+(1710)$ has a small width of 140 MeV and perhaps as small as 80 MeV.
- Both suggest the $2s$ excitation on the lattice may be insensitive to modifications of the meson dressings.
- Consider a quenched QCD simulation with matched lattice spacing and quark masses.
  - Couplings to meson dressings are suppressed.
  - Sickness: Negative-metric issues corrupt states with large meson-baryon components.

Evidence the $2s$ state is associated with the $N1/2^+(1710)$ and $N1/2^+(1880)$

- The $N1/2^+(1880)$ was observed in photoproduction while missed in πN scattering.
- The $N1/2^+(1710)$ has a small width of 140 MeV and perhaps as small as 80 MeV.
- Both suggest the $2s$ excitation on the lattice may be insensitive to modifications of the meson dressings.
- Consider a quenched QCD simulation with matched lattice spacing and quark masses.
  - Couplings to meson dressings are suppressed.
  - Sickness: Negative-metric issues corrupt states with large meson-baryon components.
- Is there a state ~ 1.9 GeV that is insensitive to quenching?

Comparison of 2+1 flavour and quenched lattice simulation results

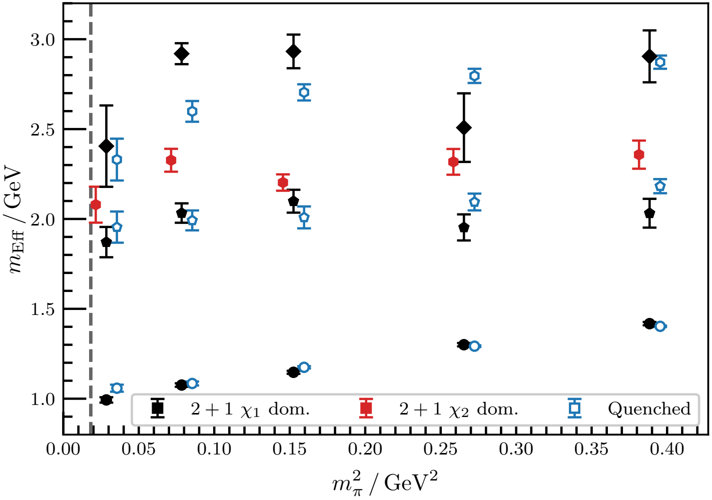

Δ-baryon spectrum from lattice QCD

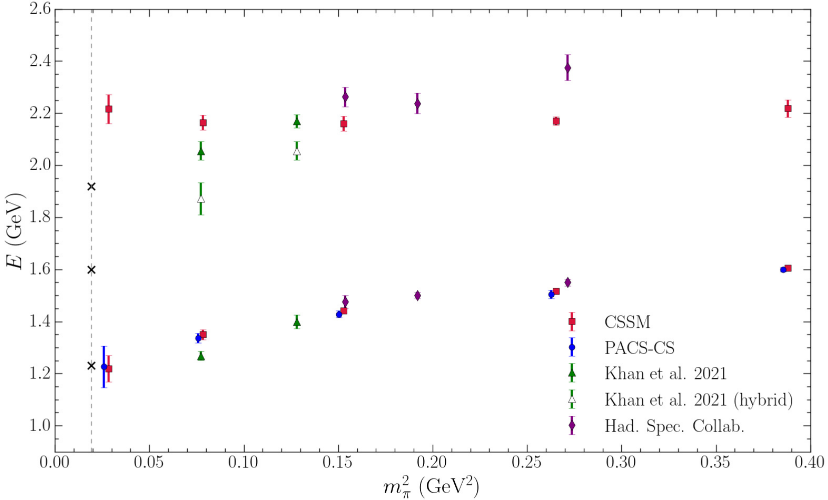

Δ-baryon spectrum from lattice QCD

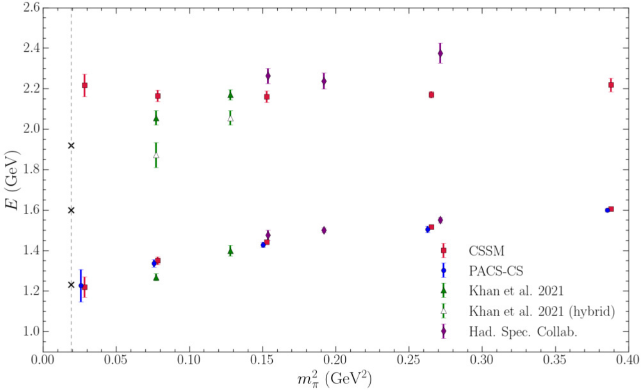

PACS-CS: S. Aoki *et al.* [PACS-CS], Phys. Rev. D **79** (2009) 034503 [arXiv:0807.1661 [hep-lat]].

Kahn ***et al.*****:** T. Khan, D. Richards and F. Winter, Phys. Rev. D **104** (2021) 034503 [arXiv:2010.03052 [hep-lat]].

Had. Spec. Collab.: J. Bulava, *et al.*, Phys. Rev. D **82** (2010) 014507 [arXiv:1004.5072 [hep-lat]].

Accessing the Radial Excitations of the Nucleon - CSSM Techniques

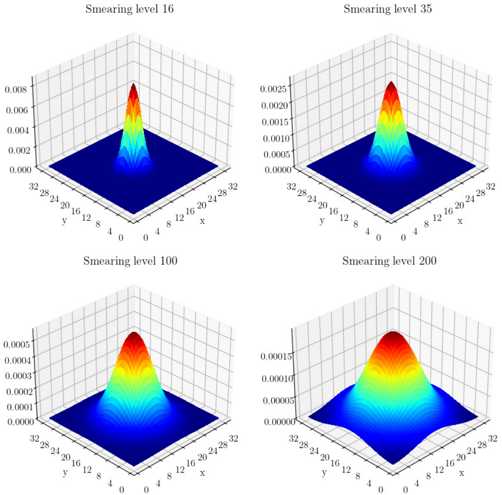

- Circa 2010.
- Local 3-quark interpolating fields.
- Quark-level source smearing techniques.

Accessing the Radial Excitations of the Nucleon - CSSM Techniques

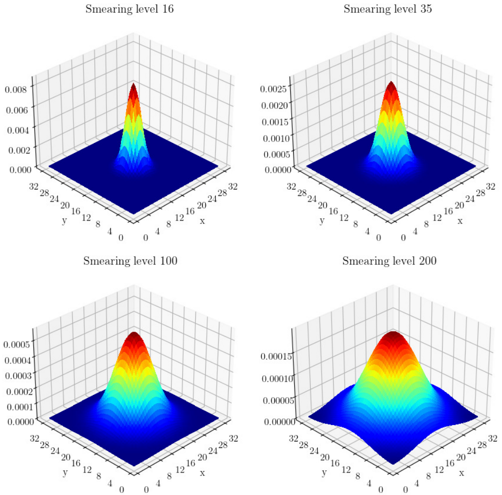

- Circa 2010.
- Local 3-quark interpolating fields.
- Quark-level source smearing techniques.
- Correlation matrix techniques
  - Identify linear combinations of sources to isolate states.
  - Opposite sign superpositions create wave function nodes.

Smeared Source Correlation Functions

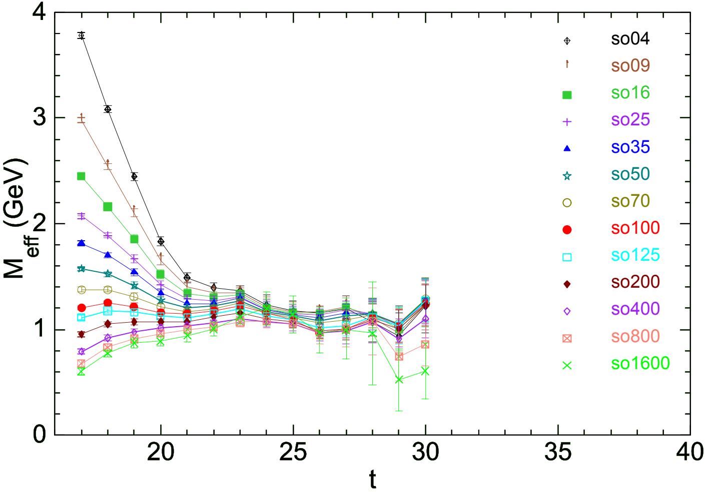

Positive Parity Nucleon Spectrum CSSM

M. S. Mahbub *et al.* [CSSM Lattice Collaboration], Phys. Lett. B **707** (2012) 389 arXiv:1011.5724 [hep-lat].

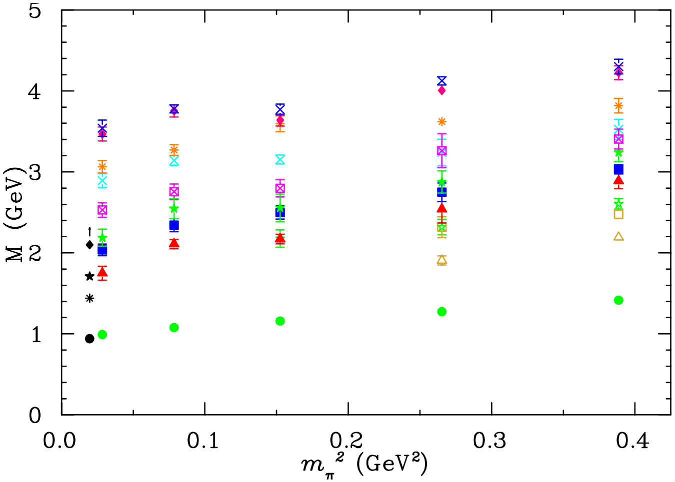

Positive Parity Nucleon Spectrum CSSM & JLab HSC

R. G. Edwards, J. J. Dudek, D. G. Richards and S. J. Wallace, Phys. Rev. D **84** (2011) 074508 arXiv:1104.5152 [hep-ph].

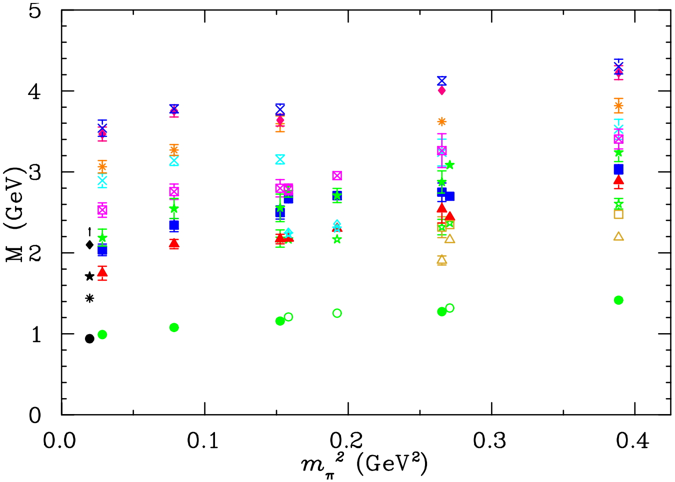

Negative Parity Nucleon Spectrum CSSM

M. S. Mahbub *et al.* [CSSM Lattice Collaboration], Phys. Lett. B **707** (2012) 389 arXiv:1011.5724 [hep-lat].

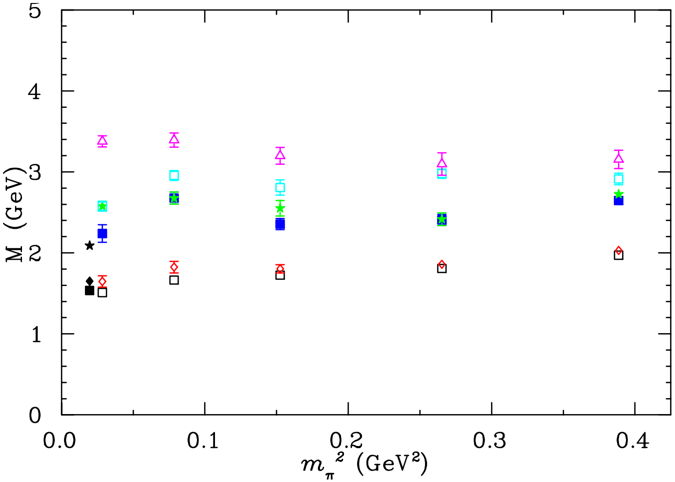

Negative Parity Nucleon Spectrum CSSM & JLab HSC

R. G. Edwards, J. J. Dudek, D. G. Richards and S. J. Wallace, Phys. Rev. D **84** (2011) 074508 arXiv:1104.5152 [hep-ph].

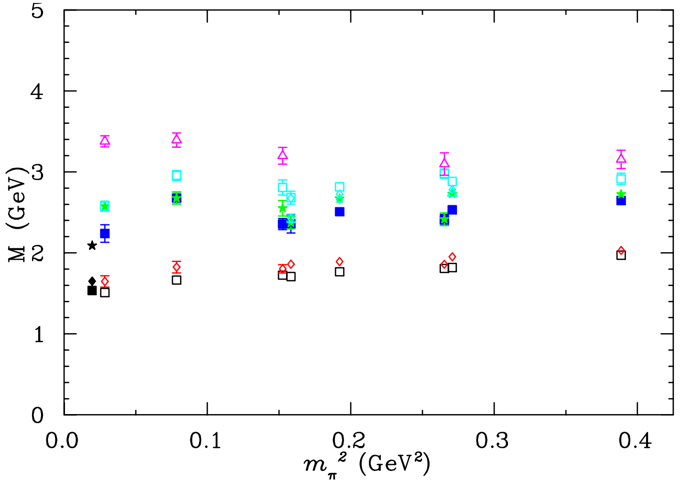

Other Calculations of the Nucleon Spectrum

- Berlin-Graz-Regensburg (BGR) collaboration

  G. P. Engel *et al.* [BGR], Phys. Rev. D **87** (2013) no.7, 074504 [arXiv:1301.4318 [hep-lat]].

  In agreement but with large uncertainties.

Other Calculations of the Nucleon Spectrum

- Berlin-Graz-Regensburg (BGR) collaboration

  G. P. Engel *et al.* [BGR], Phys. Rev. D **87** (2013) no.7, 074504 [arXiv:1301.4318 [hep-lat]].

  In agreement but with large uncertainties.

- χQCD Collaboration results

  K. F. Liu, *et al.*, "The Roper Puzzle," PoS **LATTICE2013** (2014), 507 [arXiv:1403.6847 [hep-ph]].

  Analysed the HSC correlators with their Sequential Empirical Bayesian analysis.

Other Calculations of the Nucleon Spectrum

- Berlin-Graz-Regensburg (BGR) collaboration

  G. P. Engel *et al.* [BGR], Phys. Rev. D **87** (2013) no.7, 074504 [arXiv:1301.4318 [hep-lat]].

  In agreement but with large uncertainties.

- χQCD Collaboration results

  K. F. Liu, *et al.*, "The Roper Puzzle," PoS **LATTICE2013** (2014), 507 [arXiv:1403.6847 [hep-ph]].

  Analysed the HSC correlators with their Sequential Empirical Bayesian analysis.

  - One correlator versus $28 \times 28 = 784$ correlators analysed by the HSC.

Other Calculations of the Nucleon Spectrum

- Berlin-Graz-Regensburg (BGR) collaboration

  G. P. Engel *et al.* [BGR], Phys. Rev. D **87** (2013) no.7, 074504 [arXiv:1301.4318 [hep-lat]].

  In agreement but with large uncertainties.

- χQCD Collaboration results

  K. F. Liu, *et al.*, "The Roper Puzzle," PoS **LATTICE2013** (2014), 507 [arXiv:1403.6847 [hep-ph]].

  Analysed the HSC correlators with their Sequential Empirical Bayesian analysis.
  - One correlator versus $28 \times 28 = 784$ correlators analysed by the HSC.
  - Obtained a result 300 MeV below that of the HSC.

Other Calculations of the Nucleon Spectrum

- Berlin-Graz-Regensburg (BGR) collaboration

  G. P. Engel *et al.* [BGR], Phys. Rev. D **87** (2013) no.7, 074504 [arXiv:1301.4318 [hep-lat]].

  In agreement but with large uncertainties.

- χQCD Collaboration results

  K. F. Liu, *et al.*, "The Roper Puzzle," PoS **LATTICE2013** (2014), 507 [arXiv:1403.6847 [hep-ph]].

  Analysed the HSC correlators with their Sequential Empirical Bayesian analysis.
  - One correlator versus $28 \times 28 = 784$ correlators analysed by the HSC.
  - Obtained a result 300 MeV below that of the HSC.
  - Conjectured the HSC results are wrong.
    - Their source smearing is too small to see the wave function node.

Other Calculations of the Nucleon Spectrum

- Berlin-Graz-Regensburg (BGR) collaboration

  G. P. Engel *et al.* [BGR], Phys. Rev. D **87** (2013) no.7, 074504 [arXiv:1301.4318 [hep-lat]].

  In agreement but with large uncertainties.

- χQCD Collaboration results

  K. F. Liu, *et al.*, "The Roper Puzzle," PoS **LATTICE2013** (2014), 507 [arXiv:1403.6847 [hep-ph]].

  Analysed the HSC correlators with their Sequential Empirical Bayesian analysis.
  - One correlator versus $28 \times 28 = 784$ correlators analysed by the HSC.
  - Obtained a result 300 MeV below that of the HSC.
  - Conjectured the HSC results are wrong.
    - Their source smearing is too small to see the wave function node.
  - Argument already excluded by the CSSM results.

Other Calculations of the Nucleon Spectrum

- Berlin-Graz-Regensburg (BGR) collaboration

  G. P. Engel *et al.* [BGR], Phys. Rev. D **87** (2013) no.7, 074504 [arXiv:1301.4318 [hep-lat]].

  In agreement but with large uncertainties.

- χQCD Collaboration results

  K. F. Liu, *et al.*, "The Roper Puzzle," PoS **LATTICE2013** (2014), 507 [arXiv:1403.6847 [hep-ph]].

  Analysed the HSC correlators with their Sequential Empirical Bayesian analysis.
  - One correlator versus $28 \times 28 = 784$ correlators analysed by the HSC.
  - Obtained a result 300 MeV below that of the HSC.
  - Conjectured the HSC results are wrong.
    - Their source smearing is too small to see the wave function node.
  - Argument already excluded by the CSSM results.

- Further discussion in

  D. Leinweber, *et al.* JPS Conf. Proc. **10** (2016), 010011 [arXiv:1511.09146 [hep-lat]].

Other Calculations of the Nucleon Spectrum

- Cyprus Twisted Mass and Clover Fermion results

  C. Alexandrou, *et al.*, Phys. Rev. D **89** (2014) no.3, 034502 [arXiv:1302.4410 [hep-lat]].

Other Calculations of the Nucleon Spectrum

- Cyprus Twisted Mass and Clover Fermion results

  C. Alexandrou, *et al.*, Phys. Rev. D **89** (2014) no.3, 034502 [arXiv:1302.4410 [hep-lat]].

- Correlation functions subsequently analysed in the Athens Model Independent Analysis Scheme (AMIAS).

  C. Alexandrou, *et al.*, Phys. Rev. D **91** (2015) no.1, 014506 [arXiv:1411.6765 [hep-lat]].

Positive Parity Nucleon Spectrum Circa 2017

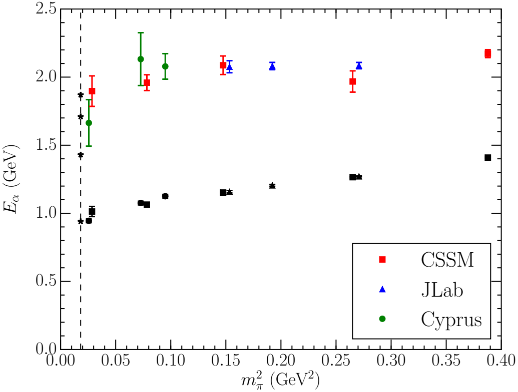

- Cyprus: C. Alexandrou, *et al.* (AMIAS), Phys. Rev. D **91**, 014506 (2015) arXiv:1411.6765 [hep-lat]
- CSSM: Z. W. Liu, *et al.* [CSSM], Phys. Rev. D **95**, 034034 (2017) arXiv:1607.04536 [nucl-th]
- JLab: R. G. Edwards, *et al.* [HSC] Phys. Rev. D **84**, 074508 (2011) [arXiv:1104.5152 [hep-ph]].

Strange Magnetic Form Factor of the $\Lambda(1405)$

J. M. M. Hall, *et al.* [CSSM], Phys. Rev. Lett. **114**, 132002 (2015) arXiv:1411.3402 [hep-lat]

- Provides direct insight into the possible dominance of a molecular $\overline{K}N$ bound state.

Strange Magnetic Form Factor of the $\Lambda(1405)$

J. M. M. Hall, *et al.* [CSSM], Phys. Rev. Lett. **114**, 132002 (2015) arXiv:1411.3402 [hep-lat]

- Provides direct insight into the possible dominance of a molecular $\overline{K}N$ bound state.
- In forming such a molecular state, the $\Lambda(u, d, s)$ valence quark configuration is complemented by
  - A $u, \overline{u}$ pair making a $K^-(s, \overline{u})$ - proton (u, u, d) bound state, or
  - A $d, \overline{d}$ pair making a $\overline{K}^0(s, \overline{d})$ - neutron (d, d, u) bound state.

Strange Magnetic Form Factor of the $\Lambda(1405)$

J. M. M. Hall, *et al.* [CSSM], Phys. Rev. Lett. **114**, 132002 (2015) arXiv:1411.3402 [hep-lat]

- Provides direct insight into the possible dominance of a molecular $\overline{K}N$ bound state.
- In forming such a molecular state, the $\Lambda(u, d, s)$ valence quark configuration is complemented by
  - A $u, \overline{u}$ pair making a $K^-(s, \overline{u})$ - proton (u, u, d) bound state, or
  - A $d, \overline{d}$ pair making a $\overline{K}^0(s, \overline{d})$ - neutron (d, d, u) bound state.
- In both cases the strange quark is confined within a spin-0 kaon and has no preferred spin orientation.

Strange Magnetic Form Factor of the $\Lambda(1405)$

J. M. M. Hall, *et al.* [CSSM], Phys. Rev. Lett. **114**, 132002 (2015) arXiv:1411.3402 [hep-lat]

- Provides direct insight into the possible dominance of a molecular $\overline{K}N$ bound state.
- In forming such a molecular state, the $\Lambda(u, d, s)$ valence quark configuration is complemented by
  - A $u, \overline{u}$ pair making a $K^-(s, \overline{u})$ - proton (u, u, d) bound state, or
  - A $d, \overline{d}$ pair making a $\overline{K}^0(s, \overline{d})$ - neutron (d, d, u) bound state.
- In both cases the strange quark is confined within a spin-0 kaon and has no preferred spin orientation.
- To conserve parity, the kaon has zero orbital angular momentum.

Strange Magnetic Form Factor of the $\Lambda(1405)$

J. M. M. Hall, *et al.* [CSSM], Phys. Rev. Lett. **114**, 132002 (2015) arXiv:1411.3402 [hep-lat]

- Provides direct insight into the possible dominance of a molecular $\overline{K}N$ bound state.
- In forming such a molecular state, the $\Lambda(u,d,s)$ valence quark configuration is complemented by
  - A $u, \overline{u}$ pair making a $K^-(s,\overline{u})$ - proton (u,u,d) bound state, or
  - A $d, \overline{d}$ pair making a $\overline{K}^0(s,\overline{d})$ - neutron (d,d,u) bound state.
- In both cases the strange quark is confined within a spin-0 kaon and has no preferred spin orientation.
- To conserve parity, the kaon has zero orbital angular momentum.
- Thus, the strange quark does not contribute to the magnetic form factor of the $\Lambda(1405)$ when it is dominated by a $\overline{K}N$ molecule.

Strange Magnetic Form Factor of the $\Lambda(1405)$

J. M. M. Hall, *et al.* [CSSM], Phys. Rev. Lett. **114**, 132002 (2015) arXiv:1411.3402 [hep-lat]